Transportation Research Part E 189 (2024) 103644

Contents lists available at ScienceDirect

Transportation Research Part E

journal homepage: www.elsevier.com/locate/tre

# Saving energy with eco-friendly routing of an electric vehicle fleet

Soomin Woo [a,d,*,1], Eric Yongkeun Choi [b], Scott J. Moura [a], Francesco Borrelli [b,c]

[a] Civil and Environmental Engineering, University of California, Berkeley, 609 Davis Hall, Berkeley, 94720, CA, USA
[b] Mechanical Engineering, University of California, Berkeley, 5133 Etcheverry Hall, Berkeley, 94720, CA, USA
[c] WideSense, Inc., Berkeley, 94720, CA, USA
[d] Smart Vehicle Engineering, Konkuk University, Seoul, 05029, Korea

ARTICLE INFO

*Keywords:*
Vehicle routing problem
Electric vehicle charging
Electric logistics
Green logistics
Energy consumption reduction
Sustainable mobility
Field experiments
Sensitivity analysis
Simulation tests
Meta-heuristic methods
Adaptive large neighborhood search
Simulated annealing

ABSTRACT

This paper fills the research gap between theoretical vehicle routing algorithms and practical solutions in the field. We use commercially developed prediction algorithms for the energy consumption of vehicles and solve for the energy-efficient routing and charging strategies of an electric vehicle fleet to visit a given set of destinations using meta-heuristics. Then we validate the energy saving performance of the efficient routing solutions with real-world vehicle measurements in a real traffic network. We also conduct a sensitivity analysis via simulation to explore some critical factors in reducing energy consumption. Current literature on vehicle routing problems is limited because they do not validate the energy consumption or the travel time of the solution in the field. This opens questions regarding the routing performance, which faces significant uncertainty from a real traffic network. Also, the travel costs in the network, such as energy consumption and travel time, have been predicted with simple or physics-based models in the theoretical studies, which are limited in capturing the complexity of a real traffic network. Our contributions are as follows. First, we develop a comprehensive framework for routing and charging an electric fleet, integrated with a high-precision prediction algorithm of energy and travel time based on learning a large driving data set. Second, we validate our routing performance in the San Francisco East Bay area with an energy consumption reduction of up to 31% compared to a baseline. Third, we conduct a sensitivity analysis via simulation on some critical constraints of vehicle routing. We observe that relaxing the limitation on operation duration and battery size on the vehicle fleet can expand the solution's feasible space and reduce the optimal energy consumption; however, the benefits diminish as constraints are relaxed to a certain point.

## 1. Introduction

This paper presents a validation of energy consumption reduction of an electric vehicle fleet by routing and driving energy-efficient routes in a real traffic network. As a solution to alleviate climate change and the energy crises, electric vehicles (EVs) can be powered by clean and renewable energy that reduce tail-pipe emissions and operate at a well-to-wheel energy efficiency of about 87 to 91% (Department of Energy, 2022a). This is higher than internal combustion engine (ICE) vehicles, which achieve

* Corresponding author.
*E-mail addresses:* soominwoo@konkuk.ac.kr (S. Woo), yk90@berkeley.edu (E.Y. Choi), smoura@berkeley.edu (S.J. Moura), fborrelli@berkeley.edu (F. Borrelli).

[1] Soomin Woo was a postdoctoral researcher at the University of California, Berkeley, during this study.

https://doi.org/10.1016/j.tre.2024.103644
Received 1 February 2024; Received in revised form 16 June 2024; Accepted 25 June 2024
Available online 15 July 2024
1366-5545/© 2024 Elsevier Ltd. All rights are reserved, including those for text and data mining, AI training, and similar technologies.

## Nomenclature

### Acronyms

| | |
|---|---|
| ALNS | Adaptive Large Neighborhood Search |
| API | Application Programming Interface |
| BEV | Battery Electric Vehicle |
| EV | Electric Vehicle |
| EVRP | Electric Vehicle Routing Problem |
| GPS | Global Positioning System |
| HVAC | Heating, ventilation, and air conditioning |
| ICE | Internal Combustion Engine |
| OFV | Objective function value |
| SA | Simulated Annealing |
| VRP | Vehicle Routing Problem |

### Decision Variables

| | |
|---|---|
| $B_i^v$ | Battery energy level of vehicle $v$ at arrival to node $i$ (kWh) |
| $b_{ij}^v$ | Battery consumption of vehicle $v$ to travel from node $i$ to node $j$ (kWh) |
| $C_i^v$ | $= 1$ if vehicle $v$ charges at node $i$, $= 0$ otherwise |
| $D_i^v$ | Cumulative distance traveled of vehicle $v$ at arrival to node $i$ (km) |
| $E_i^v$ | Charging energy of vehicle $v$ added at node $i$ (kWh) |
| $Q_i^v$ | Cargo level of vehicle $v$ at arrival to node $i$ (unit) |
| $T_i^v$ | Elapsed time of vehicle $v$ at arrival to node $i$ (hours) |
| $x_{ij}^v$ | $= 1$ if vehicle $v$ travels from node $i$ to node $j$, $= 0$ otherwise |

### Mapping Functions

| | |
|---|---|
| $A^+$ | $A^+ : T \times \tau \to T$, a function that returns new time that adds the time interval $\tau$ to given time $T$ |
| $A^-$ | $A^- : T \times \tau \to T$, a function that returns new time that subtracts the time interval $\tau$ from given time $T$ |
| $H$ | $H : T \to h$, a function that returns the hour index $h$ of given time $T$ |

### Parameters - Network

| | |
|---|---|
| $\mathcal{E}$ | Set of edges, $\mathcal{E} = \{(i,j) \mid i,j \in (V \cup D) \cup \{i = \emptyset \cap j \in (V \cup D)\} \cup \{i \in (V \cup D) \cap j = N+1\}\}$ |
| $\mathcal{G}$ | Graph consisting of the nodes and edges, $\mathcal{G} = (\{V_0, V, F, C\}, \mathcal{E})$ |
| $\overline{P_n^i}$ | Rated charging power of charger at node $i \in \{V, D, D_d\}$ |
| $\tau_f$ | Constant time cost to set up charging (hour) |
| $\tau_s^i$ | Service time at node $i \in \{V\}$ (hour) |
| $\tau_{ij}^{H(T)}$ | Travel time from node $i$ to node $j$ when departing $i$ at hour index of time $T$ (hour) |
| $D$ | Set of detour charger nodes, which are not located at destinations or depot |
| $D_d$ | Charger node at the depot |
| $d_{ij}^{H(T)}$ | Travel distance from node $i$ to node $j$ when departing $i$ at hour index of time $T$ (km) |
| $e_{ij}^{H(T)}$ | Energy consumption with a motor from node $i$ to node $j$ when departing $i$ at hour index of time $T$ (kWh) |
| $q^i$ | Load demand at node $i \in \{V\}$ (unit) |
| $V$ | Set of destination nodes, $V = \{1, \ldots, N\}$ |
| $V_0$ | Set of depot nodes, $V_0 = \{\emptyset, N+1\}$, where $\emptyset$ is the source and $N+1$ is the sink |

### Parameters - Time

| | |
|---|---|
| $\tau$ | Time interval, non-negative (hours), for example 0.7 h |
| $h$ | Hour index $\in \{0, 1, \ldots, 23\}$ |
| $T$ | Time index, for example 2022/10/22 12:23PM |

### Parameters - Vehicle

| | |
|---|---|
| $\overline{B^v}$ | Maximum battery capacity of vehicle $v$ (kWh) |
| $\overline{P_c^v}$ | Rated charging power of vehicle $v$ (kW) |

| | |
|---|---|
| $\overline{Q^v}$ | Cargo capacity of vehicle $v$ (unit) |
| $\overline{T_c^v}$ | Latest charging completion time at the depot charger for vehicle $v$ |
| $\overline{T^v}$ | Latest arrival time at the depot for vehicle $v$ |
| $B_{ini}^v$ | Initial battery level constraints of vehicle $v$ (kWh) |
| $B_{ter}^v$ | Terminal battery level constraints of vehicle $v$ (kWh) |
| $W$ | A set of vehicles in the fleet, where vehicle $v \in W$ |
| $\underline{B^v}$ | Minimum battery level of vehicle $v$ (kWh) |
| $\underline{T^v}$ | Departure time from depot for vehicle $v$ |

about 16 to 25% well-to-wheel energy efficiency (Department of Energy, 2022b). Recently, fleet operators have been adopting EVs. For example, Amazon deployed their first custom-made electric vans made by Rivian (Amazon, 2022). Operating EVs for fleets have additional benefits beyond their environmental advantages. EVs offer lower operating costs due to their enhanced fuel economy, and are particularly advantageous in scenarios involving frequent stop-and-go, which are typical for many fleet operations. Also, the relative stability of electricity prices, as apposed to the volatility of gasoline and diesel prices, provides fleet operators with more predictable energy expenses (Department of Energy, 2023b). However, transitioning fleets to EVs poses challenges because EVs have a shorter driving range than ICE vehicles, a longer charging time than refueling, and charging infrastructure is not yet ubiquitous (Department of Energy, 2023a). Therefore, fleet operators need to consider more decision variables and constraints for routing and charging EV fleets.

An Electric Vehicle Routing Problem (EVRP) is a variant of the classic Vehicle Routing Problem (VRP). VRP is a combinatorial problem whose solution performance has been advancing greatly by the operation research community as thoroughly reviewed (Moghdani et al., 2021; Kucukoglu et al., 2021; Vidal et al., 2020; Asghari and Al-e-hashem, 2021). Given a vehicle fleet, a set of destinations, and a depot, a VRP seeks to optimize an objective function by solving the assignment of destinations to each vehicle and the touring sequence of destinations while meeting the vehicle constraints, such as the driving range, total travel time, and the delivery constraints, such as the cargo load and the preferred time windows for delivery. There are many VRP variants, where an EVRP additionally solves charging decisions and models the EV costs to traverse a network. In this paper, we focus on EV fleets.

A large body of VRP literature explores energy consumption. For EVs, the remaining energy level in the battery is a critical concern because the charging infrastructure is not as ubiquitous as gas stations, and the charging takes longer. Therefore, the energy consumption of EVs must be considered to produce a vehicle routing solution that can perform successfully in practical applications. Moreover, we have technologies to investigate the energy performance of EVRPs in real life. For instance, modeling the energy consumption of EVs is easier than ICE vehicles because electric powertrains are simpler systems than internal combustion engines (Butler et al., 1999). Additionally, the vehicle battery is equipped with sensors that digitize its information (Basu et al., 2018). Even with its needs and opportunities, however, the current literature lacks to validate the energy performance of EVRP solutions in the real-world, therefore supporting their claims on successful modeling or improvements on the energy performance. In the following, we provide a literature review that considers the energy aspect of EVRPs, but with no validation of energy consumption in the field.

Many studies on VRPs use theoretical and simple energy consumption models, often as a function of travel time or distance. Montoya et al. and Koyuncu et al. assume constant travel time and energy consumption values for each edge in the network for an electric vehicle routing and charging problem (Montoya et al., 2017; Koyuncu and Yavuz, 2019). Catay et al. estimate energy consumption to be proportional to travel distance and minimize energy costs of an EV fleet with various charging types in the network (Catay and Keskin, 2017). Kopfer et al. minimize total energy consumption for a heterogeneous fleet of ICE vehicles and EVs (Kopfer and Vornhusen, 2018). They use constant values for travel time and distance in their transportation network and estimate energy consumption as a function of distance and weight and assume constant average velocity. Hiermann et al. minimize the total cost of a heterogeneous fleet with ICE, EVs, and hybrid electric vehicles, including the charging and fuel costs (Hiermann et al., 2019). They estimate the battery and fuel consumption as linear functions of constant travel distances and efficiency rates. Ferro et al. minimize the cost of total travel distance and energy purchase cost for EVs, using a time-varying price of electricity (Ferro et al., 2018). They model energy consumption as a function of slope, mass, speed, drive efficiency, power converter efficiency, and rolling friction coefficient. Lin et al. minimize the electricity cost of EVs by routing and scheduling the charge and discharge to the grid with respect to time-varying electricity cost (Lin et al., 2021). They model energy consumption as a linear function of the constant travel distance and energy consumption rate, though the energy cost is more complex due to the time-varying electricity price. Kim et al. minimize the total energy consumption of electric vehicles with energy consumption that linearly depends on the vehicle battery level (or State-of-Charge) (Kim and Chung, 2023). They conduct numerical experiments, varying the coefficient values of the energy consumption model. Bruglieri et al. minimize the total cost (including the cost of energy consumed) by modeling linear relationships of energy consumption rate with the payload and the vehicle speed and considering en-route stops to the recharging stations (Bruglieri et al., 2023). They provide a numerical study on their solution's performance. Zhang et al. minimize the total operation cost of an electric fleet of ride-sharing vehicles (Zhang et al., 2024b). This study uses a commercially available Baidu Map Application Programming Interface (API) to extract realistic information on the travel time and distance in real-world

traffic, however, the data on energy consumption data for the numerical experiment is not described. Zhang et al. optimize the on-demand bus routing problem using real-world data of bus lines in Beijing (Zhang et al., 2024a). They use a map API to extract driving time data, but simplify the modeling of energy consumption with a proxy of time duration that the bus can travel with its current remaining battery energy.

Some literature adopts more sophisticated models of energy consumption for vehicle routing. However, most studies described in the following validate their routing results by network simulation, if not noted otherwise. Guanetti et al. minimize the energy consumption of plug-in hybrid electric vehicles, estimated by integrating the instantaneous mechanic power at the wheel with velocity information acquired from traffic APIs (Guanetti et al., 2019). Basso et al. minimize the energy consumption of an EV fleet for routing and charging decisions, assuming free flow and constant speed and using Volvo's high fidelity vehicle simulator to estimate the energy consumption (Basso et al., 2019). Basso et al. improve their previous work and use a time-dependent speed of road links by dividing the day into 24 periods and simulating the traffic with SUMO (Basso et al., 2021). The energy estimation is validated by field data from non-EV buses and the simulation of electric trucks with Volvo's high-fidelity vehicle simulator. Their routing result is validated by simulation. Macrina et al. estimate the energy consumption of ICE vehicles and EVs with different speed values for the edges in the network, payload, and road gradient, but assume constant travel times with no traffic congestion (Macrina et al., 2019). De Nunzio et al. minimize the energy consumption for routing a single vehicle, such as an EV, an ICE vehicle, or a hybrid electric vehicle, without charging (Nunzio et al., 2021). They model the energy consumption based on vehicle powertrain, acceleration, velocity, and road grade. However, the speed of a road segment is calculated with a constant acceleration. Lu et al. minimize the total cost of an EV fleet including the energy cost, while modeling the energy consumption with time-dependent speeds on each edge, vehicle mass, and distance, but no acceleration (Lu et al., 2020). Bahrami et al. minimize the total gasoline consumption of plug-in hybrid electric vehicles and optimize the battery energy and fuel consumption on a given path between two nodes using the driving cycle profile acquired from driving data in Toronto Bahrami et al. (2020). The routing performance was evaluated through simulation with a case study in Toronto. Peng et al. (2023) propose energy-efficient dispatching of electric truck fleets. They model the energy consumption in terms of the travel distance, vehicle mass, and acceleration and compare the energy performance of the proposed routing strategy with a baseline routing solution used by the logistics company. However, their numerical experiments do not validate the energy performance in the field and they ignore the impact of real world traffic conditions, such as road grade, dynamic traffic congestion, and weather.

We identify three research gaps in the current literature, despite the extensive work on modeling and solving VRPs and their variants. First, to the best of our knowledge, no study has developed a vehicle routing solution and validated the routing performance in the field. The current studies rely on the simulation of travel costs in the network and evaluate the solution performance without capturing the actual uncertainties of a real traffic network, including traffic congestion, travel delays, and more. Some works validate the energy cost models in the field, but no field experiments analyze an optimized route found by the algorithm and compare against a baseline. This fact represents a severe disconnection between the vehicle routing algorithm literature and practical application. The solutions have been tested for optimality and computation times only in simulation. How the solutions perform in real life has been left unknown.

Second, the travel costs, such as travel time and energy consumption, are very challenging to measure and predict due to the uncertain factors in real traffic, such as traffic speed, ambient temperature, air conditioning, road grade, driving behavior, and unexpected events. Energy consumption is even more challenging to predict than travel time because of a lack of available data. However, with the adoption of on-board sensors in vehicle batteries and connected vehicle technologies that send various signals to the cloud, we can gather rich sets of driving data in the field, including EV energy consumption. A learning algorithm can use these new data sources to model energy consumption, capture the uncertainties in real-world traffic, and improve the travel cost prediction accuracy for vehicle routing algorithms.

Third, most studies on VRPs assume a fixed path between one node to another, i.e., assuming the same roads and turns to take. However, the traffic conditions that vary dramatically over a day can change the most efficient path. For instance, in off-peak traffic, the fastest path from one node to another may use a freeway, while in peak traffic, the fastest path may take an arterial road to avoid freeway congestion. It is more realistic to adjust the path to travel an edge in the network in practice, which is done in online navigation services. However, most studies do not consider the possibility of time-varying efficient paths between nodes and do not integrate online navigation and traffic databases into the network cost estimation.

### *1.1. Research contribution*

This study fills the gap between theoretical vehicle routing algorithms and practical solutions. We contribute to the literature as follows.

1. We present a comprehensive framework for dispatching an electric fleet in the real world by high-precision algorithms to predict energy consumption across navigation paths that vary with time and traffic conditions.
2. We validate that an efficient electric vehicle routing solution reduces energy consumption by 31.4% compared to a baseline routing solution to minimize travel time via field experiments.
3. We conduct a sensitivity analysis by simulation on some critical factors, namely the time and battery constraints of the vehicle fleet. This provides new insights on how to reduce energy consumption in electric vehicle fleets.

Note that this research does not focus on the algorithmic advancement of vehicle routing solutions on their performance, such as computation time or solution optimality. These topics are studied extensively in the operations research community. In this paper,

we adopt a state-of-the-art solution approach for a VRP and modify it appropriately to suit our needs for solving an electric vehicle routing and charging problem. Although we will describe our solution algorithm in detail, there is a large body of literature and review papers that comprehensively describe solution algorithms; please refer to Moghdani et al. (2021), Kucukoglu et al. (2021), Vidal et al. (2020) and Asghari and Al-e-hashem (2021). Note that prediction algorithm for energy consumption of vehicles is proprietary and its details cannot be disclosed on this manuscript. Our primary focus in this paper is to show the viability of an energy-efficient vehicle routing algorithm integrated with high-precision energy estimation algorithms via field tests.

The paper is organized as follows. Section 2 details the methodology of this research, including the context of an electric vehicle fleet routing problem, the derivation of the problem formulation, and the meta-heuristic solution algorithm. Section 3 describes the field test methodology and results that show the energy savings of energy-minimizing routes in real-world traffic. Section 4 describes the sensitivity analysis of energy saving performance that varies with essential factors, such as time and battery constraints. Section 5 summarizes this paper's contributions and discusses potential future works. Note that the appendix in Appendix A is extensive, covering the details of meta-heuristic solver, the comprehensive presentation of the field test results, and additional findings from the simulation studies.

## 2. Methodology

This section describes the problem context and formulation for routing and charging an electric vehicle fleet. We explain the solution framework that uses Adaptive Large Neighborhood Search (ALNS) and Simulated Annealing (SA), the charging dynamics modeling, and the travel cost estimation. For the definition of acronyms, variables, and parameters, please refer to the Nomenclature.

### *2.1. Problem context*

We consider a heterogeneous fleet of EVs with varying capacities and a network composed of one depot, a set of destinations, and a set of heterogeneous chargers, which can be located at the depot ('depot charger'), the destinations ('destination charger'), or away from depot or destinations and thus requires a detour to visit ('detour charger'). For each edge between any pair of network nodes, time-varying costs exist in terms of travel time, energy consumption, and distance. The decision variables are the assignment of destinations and chargers, the sequence of destinations and chargers to visit, and the charging time and power for each vehicle in the fleet. The problem can minimize either the total energy consumption of the fleet or the total travel time of the fleet.

The total number of vehicles is fixed, and each vehicle may have different parameters, such as battery limits (minimum, maximum, initial, and terminal energy levels in kWh), charging power limit, cargo capacity, and time limits (departure time at the depot, latest arrival time at the depot, and latest charging end time at the depot). All dispatched vehicles must depart from and return to the depot. All destinations have non-zero cargo demand and take a fixed service time for a visit. A subset of the vehicle fleet must cover all destinations exactly once, and satisfy the physical limitations of the vehicle battery, cargo, and charging, as well as the fleet operating hours and the cargo demand of each destination. The vehicles must arrive back at the depot by the latest arrival time at the depot. However, the vehicles may continue charging at the depot charger to meet the terminal battery level constraint until the latest charging end time, which may be later than the latest arrival time.

A charging event requires a charging time, which is a function of the charging energy and the power capacities of the vehicle and the charger, in addition to a fixed time of 5 min to initiate charging. The chargers are heterogeneous and vary in their power capacities. We assume no queue at a charger. A vehicle may visit the same detour charger or the depot charger multiple times, and multiple vehicles can visit the same detour charger or the depot charger. A destination charger can be visited at most once by one vehicle. The number of charging visits is designed with the following assumptions. First, the fleet operator may have a partnership with a network of public chargers (modeled as detour chargers). They may be equipped with fast chargers, sufficient space for fleet vehicles, as well as rest areas for drivers, with high charging service quality. Therefore, multiple visits are reasonable to the detour chargers. Second, we restrict the visits to destination chargers to reduce visiting the possibly busy area near destinations, occupying the parking or loading zones.

We consider the travel costs to be time-dependent. The energy consumption and the travel time can vary by the hour due to traffic conditions. Also, the travel distance from one location to another can change with time because the efficient paths (perhaps recommended by online navigation services) can vary depending on the real-time traffic conditions. We use the values of travel time, energy consumption, and distance of a travel path from one location to another that varies each hour. With time-dependent travel costs, the algorithm can reflect the different routing performances during typical working hours, for example, 6 AM to 8 PM, and during overnight hours, for example, 8 PM to 6 AM the next day. Note that we consider time progression within the solution; for example, a solution for a vehicle to travel from 2 PM to 4 PM computes the total travel time reflecting the traffic where the vehicle is at 2 PM, 3 PM, and 4 PM.

### *2.2. Problem formulation*

A vehicle routing problem is NP-hard, and the decision vector's dimension increases exponentially with the network size. As we will describe in Section 2.3, we use an approximate solution approach that efficiently solves a nonlinear problem with high complexity. In the following, we describe the mathematical formulation of our EV fleet dispatching problem. Note that the decision variables, parameters, and mapping functions are defined in the Nomenclature section.

### 2.2.1. Objective functions

In this work, we consider two objective functions for optimized fleet routing and charging. Namely, we minimize the total energy consumption $J_E$ described in Eq. (1) and the total travel time $J_T$ described in Eq. (2).

$$J_E = \sum_{v \in W} \left[ B_{\emptyset}^{v} - B_{N+1}^{v} + \sum_{i \in V_0 \cup V \cup D} E_i^v \right] \tag{1}$$

$$J_T = \sum_{v \in W} T_{N+1}^{v} - T_{\emptyset}^{v} \tag{2}$$

For $J_E$, we use for all vehicles $v$, the difference between the battery energy level at departure from the depot, $B_{\emptyset}^{v}$ and that at arrival back at the depot $B_{N+1}^{v}$, accounting the charging energy at each visit on the route, $E_i^v$. Note that this calculates the consumption only. For $J_T$, we use for all vehicles $v$, the difference between the elapsed time at the return to the depot $T_{N+1}^{v}$ and that at the departure from the depot $T_{\emptyset}^{v}$.

### 2.2.2. Constraints

The constraints of this problem are formulated in complex and nonlinear expressions that are easily solved using approximation methods with highly efficient solutions. We can group the constraints largely into the network and travel cost constraints, the vehicle energy consumption constraints, the charging decision constraints, the initial and terminal conditions, the physical capacities of vehicles, and the variable domain constraints.

First, we have the network flow and travel cost constraints as the following.

$$\sum_{v} \sum_{\forall j \neq i} x_{ij}^{v} = 1 \qquad \forall i \in V \tag{3}$$

$$\sum_{v} \sum_{\forall i \in \{\{\emptyset\} \cup V \cup D\} \neq j} x_{ij}^{v} - \sum_{v} \sum_{\forall i \in \{\{N+1\} \cup V \cup D\} \neq j} x_{ji}^{v} = 0 \qquad \forall j \in \{V, D\} \tag{4}$$

$$T_j^v = x_{ij}^v \left[ A^+ \left( T_i^v, \quad \tau_s^i + \tau_{ij}^{H(T_i^v)} + E_i^v \cdot \min\left\{ \overline{P_c^v}, \overline{P_n^i} \right\}^{-1} + \tau_f C_i^v \right) \right] \qquad \forall v \in W, \quad \forall i,j \in \{V_0, V, D\} \tag{5}$$

$$B_j^v = x_{ij}^v [B_i^v - b_{ij}^v + E_i^v] \qquad \forall v \in W, \quad \forall i,j \in \{V_0, V, D\} \tag{6}$$

$$D_j^v = x_{ij}^v \left[ D_i^v + d_{ij}^{H(t_i^v)} \right] \qquad \forall v \in W, \quad \forall i,j \in \{V_0, V, D\} \tag{7}$$

$$Q_j^v = x_{ij}^v \left[ Q_i^v + q^i \right] \qquad \forall v \in W, \quad \forall i,j \in \{V_0, V, D\} \tag{8}$$

Eq. (3) ensures that all destinations are visited exactly once, using the binary decision variable $x_{ij}^v$ that equals 1 if vehicle $v$ travels from node $i$ to node $j$, and 0 otherwise. Eq. (4) reflects the flow conservation in the network. Eq. (5) computes the travel time of vehicle $v$ at each node $j$, $T_j^v$, considering the service time, $\tau_s^i$, the travel time depending on the departure time from the previous location, $\tau_{ij}^{H(T_i^v)}$, the charging time calculated by the charging energy $E_i^v$ at the node, the rated charging power of the vehicle $\overline{P_c^v}$, and the rated charging power of the charger at the node $\overline{P_n^i}$, and the fixed set-up time for charging, $\tau_f$ if the vehicle charges at the node (and $C_i^v$ will equal 1 if so, and 0 otherwise.) Note that the mapping function $A^+$ is used to add time. Eq. (6) computes the battery energy level of vehicle $v$ at arrival to node $j$, $B_i^v$, considering the battery consumption to travel, $b_{ij}^v$, and the charging energy at the previous node $i$. Eq. (7) computes the cumulative distance traveled, $D_i^v$. Note that the travel distance from node $i$ to $j$, $d_{ij}^{H(T)}$, varies with time $t_i^v$ because the recommended route can vary with the traffic condition. Eq. (8) computes the cargo load of the vehicle $v$ at arrival to node $j$, $Q_i^v$, by cumulatively adding the load demand at node $i$, $q^i$.

Second, we model the energy consumption from the motors for the battery EVs as follows.

$$b_{ij}^v \geq x_{ij}^v e_{ij}^{H(t_i^v)} \qquad \forall v \in W, \quad \forall i,j \in \{V_0, V, D\} \tag{9}$$

Eq. (9) calculates $b_{ij}^v$, the energy consumption from node $i$ to $j$ if the vehicle $v$ departs node $i$ at time $t_i^v$ to reach node $j$. Note that the energy consumption $e_{ij}^{H(t_i^v)}$ varies with time $t_i^v$ due to the time-varying traffic conditions..

Third, we model the charging energy at each destination in set $V$ or detour charger in set $D$ as the following.

$$E_i^v \leq C_i^v \cdot \min\left\{ \overline{P_c^v}, \overline{P_n^i} \right\} \left[ \overline{T^v} - \sum_k \sum_q x_{kq}^v \left( \tau_s^k + \tau_{kq}^{H(T_k^v)} \right) - \sum_{q \neq i} \left[ C_q^v \tau_f + E_q^v \cdot \min\left\{ \overline{P_n^v}, \overline{P_c^q} \right\}^{-1} \right] \right] \tag{10}$$
$$\forall v \in W, \quad \forall i \in \{V_0, V, D, D_d\}$$

$$E_i^v \leq C_i^v [\overline{B^v} - B_i^v] \qquad \forall v \in W, \quad \forall i \in \{V_0, V, D, D_d\} \tag{11}$$

$$E_i^v \leq C_i^v \cdot \max\left\{ 0, \quad \max\left\{ \underline{B^v}, B_{ter}^v \right\} - B_{ini}^v + \sum_k \sum_j x_{kj}^v e_{kj}^{H(t_k^v)} - \sum_{q \neq i} E_q^v \right\} \tag{12}$$
$$\forall v \in W, \quad \forall i \in \{V_0, V, D, D_d\}$$

Eqs. (10), (11), and (12) compute the charging energy $E_i^v$ as a minimum of three quantities shown as the right-hand sides. Eq. (10) calculates the energy that can be charged with respect to the charging time available on the route. We consider the available time by subtracting from the latest arrival time at the depot, $\overline{T^v}$, the service time and travel time (in the first summation expression) and the charging time (in the second summation expression) at other nodes on the route. The right-hand side of Eq. (10) becomes zero when there is no charging at node $i$ due to the variable $C_i^v$. Eq. (11) calculates the energy that can be charged up to the battery energy capacity, $\overline{B^v}$, at the current battery level, $B_i^v$. Eq. (12) calculates the charging energy necessary to meet the minimum and/or the terminal battery energy level. We calculate this by targeting the energy as the minimum battery level of vehicle $v$ at all times, $\underline{B^v}$, or the terminal battery level, $B_{ter}^v$. Then we subtract the initially available energy in the vehicle, $B_{ini}^v$, add the energy consumption on the route by summing $e_{kj}^{H(t_k^v)}$ appropriately, and subtract the energy charged on the route by summing $E_q^v$ appropriately. Note that the minimum battery level reflects the physical battery limit of the vehicle, while the terminal level reflects the operational constraint that the operator may want to pose on the vehicle for robustness and safety.

Fourth, we have the initial and terminal constraints as the following.

$$T_{\emptyset}^v = \underline{T^v} \qquad \forall v \in W \tag{13}$$

$$B_{\emptyset}^v = B_{ini}^v \qquad \forall v \in W \tag{14}$$

$$Q_{\emptyset}^v = 0 \qquad \forall v \in W \tag{15}$$

$$D_{\emptyset}^v = 0 \qquad \forall v \in W \tag{16}$$

Eqs. (13), (14), (15), and (16) set the departure time from the depot at $\underline{T^v}$, initial battery level at $B_{ini}^v$, initial cargo load level at 0, and initial level of cumulative distance traveled at 0, respectively, for each vehicle $v$ in the fleet.

$$T_{N+1}^v = \overline{T^v} \qquad \forall v \in W \tag{17}$$

$$\left[B_{ter}^v - B_{N+1}^v\right] \le \min\left\{\overline{P_c^v}, \overline{P_n^{D_d}}\right\}\left[\overline{T_c^v} - T_{N+1}^v\right] \qquad \forall v \in W \tag{18}$$

Eq. (17) requires the vehicle to arrive by the latest arrival time to the depot $\overline{T^v}$. Eq. (18) calculates the charging energy at the depot charger after returning to the depot. On the left-hand side, it calculates the energy required to meet the terminal battery level for vehicle $v$, $B_{ter}^v$, given that the arrival battery at the return to the depot is $B_{N+1}^v$. On the right-hand side, it calculates the energy that can be charged with the charging power capacities of vehicle and charger, $\overline{P_c^v}$ and $\overline{P_n^{D_d}}$, respectively, and the difference between the latest charging completion time, $\overline{T_c^v}$, and the vehicle's arrival time at the depot, $T_{N+1}^v$. Note that the latest charging completion time, $\overline{T_c^v}$, must be chosen equal or later than the latest arrival time at the depot $\overline{T^v}$. This research omits the time window constraints for each destination, for which we recommend the readers on the current literature, such as (Bruglieri et al., 2023; Macrina et al., 2019; Peng et al., 2023; Keskin and Çatay, 2016).

Fifth, we have the physical limitations as the following.

$$\underline{B^v} \le B_i^v \le \overline{B^v} \qquad \forall v \in W, \quad \forall i \in \{V_0, V, D\} \tag{19}$$

$$Q_i^v \le \overline{Q^v} \qquad \forall v \in W, \quad \forall i \in \{V_0, V, D\} \tag{20}$$

Eq. (19) constrains each vehicle's lower and upper limits on battery capacity, $\underline{B^v}$ and $\overline{B^v}$, respectively. Eq. (20) constrains the cargo load capacity, $\overline{Q^v}$.

Finally, we have the binary domain constraints of some decision variables as shown in Eq. (21) below.

$$x_{ij}^v, C_i^v \in \{0, 1\} \qquad \forall i, j \in \{V_0, V, D\}, \quad \forall v \in W. \tag{21}$$

### 2.3. Solution using meta-heuristics

In this paper, we choose to use a meta-heuristic method for three reasons. First, the meta-heuristic method can typically yield a high-quality solution for problems of various complexities in a practical computation time. Exact solution methods may easily fail to solve this problem. Second, the meta-heuristic method is scalable in the sense that we can easily generalize the problem instances for various fleet specifications and operation scenarios by engineering the feasibility criteria during the solution search. Third, the meta-heuristic method allows modeling flexibility using heuristic methods to modify the solution during the search. For example, we can design various heuristics to search for the charging location and energy values, and implement our insights to guide the search. This approach aligns with our wish to contribute to improving the energy efficiency of electric fleets immediately in the market.

Among the many algorithms in the meta-heuristic category, we choose Adaptive Large Neighborhood Search (ALNS) and Simulated Annealing (SA) as they are extensively used in the literature (Elshaer and Awad, 2020). In the following, we describe the solution framework and explain the algorithm, including ALNS and SA. In addition, we describe how we estimate the time-varying costs to travel in the real-world network using a high-precision prediction API serviced by WideSense.[2] Please refer to the Appendix A for the details of heuristic methods that are borrowed from the current literature and newly proposed for our specific problem in this paper.

[2] https://www.widesense.net.

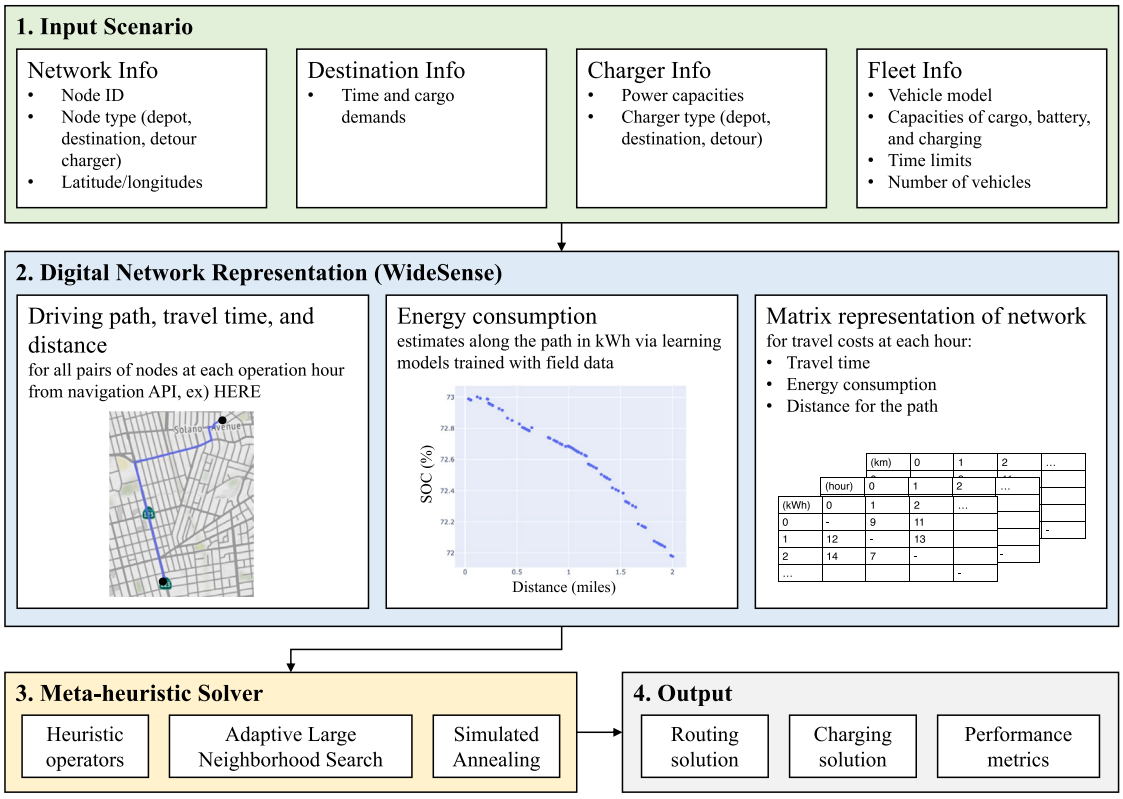


**Fig. 1.** Solution framework.

### 2.3.1. Solution framework

We briefly describe the solution framework; refer to Fig. 1. First, we prepare the input that describes the dispatching scenario, including information of the network, the destinations, the chargers, and the fleet. Second, we create a digital representation of the network. For all pairs of nodes in the network and each hour of operation, we find the driving path, travel distance, and expected travel time by navigation services like HERE API. We also estimate the energy consumption along that driving path, whose model is described in detail in Section 2.3.4. We represent the travel costs, i.e., travel distance, travel time, and energy consumption, for all pairs of edges for each hour in matrices. Third, the meta-heuristic algorithm using ALNS and SA solves the problem. Finally, the framework outputs the routing and charging solution computed in a given time and the performance metrics.

### 2.3.2. Meta-heuristic algorithm

We describe the meta-heuristic algorithm, corresponding to the third box in Fig. 1, with Algorithm 1. Note that the parameter values used in this study are given at the end of this subsection. From line 1 to 3, we initialize the routing and charging solution by simple heuristics, such as a greedy algorithm, calculate its objective function value (OFV), and set this solution as the current and the best solution. We initialize the temperature for SA, $T_{SA}$ as $T_{SA}^{init}$, and the iteration number $i$ to zero. We create a pool of heuristic methods composed of destroy and repair operators and initialize their weights $w_{op}$ and scores $s$ as zero for ALNS. We record the starting time of computation.

We start the iterations of ALNS at line 4, which stops when the iteration or computation time limit is reached. At each iteration, we generate a candidate solution from line 5 to 14 by modifying the current solution. We will only modify a particular aspect of the solution, such as the detour chargers, an entire route, or some destinations, depending on a random sampling of $r$ from a uniform distribution. For the selected aspect, we select one destroy operator and one repair operator based on another random sampling with probability as the operators' weights. The weights are accumulated scores representing how well the operators have performed in the past iterations. The operators are selected randomly when the weights are initialized as zeros. We 'destroy' and 'repair' the current solution with the selected operators to produce a candidate solution and evaluate its OFV. If any route is infeasible, then we execute the charging decision algorithm (explained later in Section 2.3.3) on the route.

Next, we use the SA criterion to decide if we accept the candidate solution as current from line 15 to line 24. If the candidate solution visits more destinations or uses fewer vehicles than the current, we accept the candidate. Also, if the candidate uses the same number of vehicles but has a smaller OFV, we accept the candidate. We reject the candidate if the candidate uses more vehicles than the current. If the decision is not made under these conditions, the SA criteria selects the candidate as the current

**Algorithm 1:** Meta-heuristic Algorithm using ALNS and SA

**Input:** Information on network, destinations, chargers, and vehicle fleet
**Result:** The visiting order to the assigned nodes, charging time, and charging energy for each vehicle

Generate an initial solution as the current solution and the best solution, and record its OFV;
Initialize the hyper-parameters, $T_{SA} \leftarrow T_{SA}^{init}$, $i \leftarrow 0$, $s \leftarrow 0$, and $w_{op} \leftarrow 0$ for all operators;
Record the current time of computation $t_{\text{curr}}$ as the starting time $t_{\text{init}}$;
**while** $i < i_{max}$ *and* $t_{curr} - t_{init} < t_{max}$ **do**
    /* Generate a candidate solution with destroy and repair operators */
    $r \leftarrow$ random sampling from a uniform distribution $U[0, 1]$;
    **if** $r \in [0, r_{CD}]$ **then**
        Select and apply detour charger destroy/insertion operators to modify the solution;
    **else if** $r \in (r_{CD}, r_{CD} + r_{RD}]$ **then**
        Select and apply route destroy/insertion operators to modify the solution;
    **else**
        Select and apply destination destroy/insertion operators to modify the solution;
    Evaluate feasibility and OFV of the candidate solution;
    **if** *any route is infeasible in the candidate solution* **then**
        Adjust charging decisions by Algorithm 2 on the modified route(s);
    /* Evaluate the candidate solution compared to the current solution */
    **if** *the candidate visits more destinations than the current* **then**
        DECISION $\leftarrow$ ACCEPT;
    **else if** *the candidate uses fewer vehicles than the current* **then**
        DECISION $\leftarrow$ ACCEPT;
    **else if** *the candidate uses the same number of vehicles but at a smaller OFV* **then**
        DECISION $\leftarrow$ ACCEPT;
    **else if** *the candidate uses more vehicles than the current* **then**
        DECISION $\leftarrow$ REJECT;
    **else**
        Accept or reject the candidate solution based on SA, and update $T_{SA}$;
    /* Update the current solution and select the operator score */
    **if** *DECISION* $=$ *ACCEPT* **then**
        Current solution $\leftarrow$ candidate solution;
        **if** $OFV_{cand} < OFV_{curr}$ **then**
            $s = S_{\text{better}}$;
            **if** $OFV_{cand} < OFV_{best}$ *and the candidate solution is feasible* **then**
                $s = S_{\text{best}}$;
                Best solution $\leftarrow$ candidate solution;
        **else**
            $s = S_{\text{accept}}$;
    **else**
        $s = S_{\text{reject}}$;
    /* Update the weights of destroy and repair operators with the score */
    Add the score $s$ to the chosen destroy and repair operators;
    **if** $r \in [0, r_{CD} + r_{RD}]$ **then**
        Update the current weights of the detour charger or route operators, $w_{op}$, with decay as $w_{op} \leftarrow d \cdot w_{op} + (1 - d) \cdot s$ ;
    **else if** $i \mod i_{seg} = 0$ **then**
        Update current weights for the destination destroy/repair operators using segment decay ;
    Update the current time at computation, $t_{curr}$, and $i \leftarrow i + 1$ ;
Return the best solution;

with probability, $\exp\left(\frac{OFV_{curr} - OFV_{cand}}{T_{SA}}\right)$, where $OFV_{curr}$ and $OFV_{cand}$ are the OFVs of current and candidate solutions, respectively. Given the same values of current and candidate solution values, the exponential probability function is higher at a high temperature $T_{SA}$. In other words, we are more likely to accept a candidate solution with a higher OFV at a higher temperature, exploring the solution space ambitiously. We update the temperature $T_{SA}$ with $\max\{T_{end}, T_{SA} \cdot \delta_{SA}\}$, where $T_{end}$ is the ending temperature and $\delta_{SA}$ is an increment step less than 1. This method gradually decreases $T_{SA}$, making more conservative decisions on solution acceptance and converging to local minima as iteration progresses.

The process from line 25 to 35 is briefly explained here. If we accept the candidate solution, we select a score and add it to update the weights of the used operators. The score, $s$, is selected out of four options ($S_{\text{best}}$, $S_{\text{better}}$, $S_{\text{accept}}$, and $S_{\text{reject}}$) depending the OFVs of the candidate, the current, and the best solutions. $S_{\text{best}}$ is the highest and chosen if the candidate replaces the best so far, i.e., the candidate has a better OFV than the best solution. $S_{\text{better}}$ is the second highest and chosen if the candidate replaces the current, i.e., the candidate has a better OFV than the current but not better than the best. $S_{\text{accept}}$ is the third highest and chosen if the candidate replaces the current by chance, i.e., the candidate has a worse OFV than the current and the best. $S_{\text{reject}}$ is the lowest and chosen if the candidate is rejected to be the current solution.

To record the performance of operators, we update the weights of the destroy and repair operators with the score, $s$, as shown in line 36 to 40. We use a weight decay of operators, $d$, to update the weights for the detour charger and route operators. We use a segment weight decay borrowed from Keskin and Çatay (2016) for the destination operators. Finally, we update the current computation time and the iteration number. When the iterations stop, we return the best solution so far.

We share the ALNS and SA parameters used in this study, many borrowed from Keskin and Çatay (2016). For the SA, the initial temperature is chosen as $T_{SA}^{init} = -0.12 \cdot OFV_{init} \cdot \log(0.5)^{-1}$, where $OFV_{init}$ is the OFV of the initial solution, the ending temperature is $T_{end} = 0.01$, and the increment step of SA is $\delta_{SA} = 0.9994$. For the ALNS, the maximum iteration number is $i_{max} = 15{,}000$, the maximum computation time is $t_{max} = 30$ min, the selection probability of detour charger operator is $r_{CD} = 0.15$, the selection probability of route operator is $r_{RD} = 0.10$, the weight decay of operators is $d = 0.9$, and the initial weights of operators $w_{op}$ is zero for all. The weights are $S_{\text{best}} = 25$, $S_{\text{better}} = 20$, $S_{\text{accept}} = 6$, and $S_{\text{reject}} = 0$, The segment weight decay described in Keskin and Çatay (2016) is borrowed as $(1 - \rho) = 0.75$, segment update length is $i_{seg} = 100$ though not explicitly stated in the algorithm pseudo-code.

Please find in the Appendix A the heuristic operators used in this paper. They include ones borrowed from the literature, as well as additional operators we newly propose in this paper.

The proposed model is developed in Python and computed via a Macbook Pro with 2.6 GHz 6-Core Intel Core i7 with 16 GB memory. For the field test results in Section 3, the algorithm computes for about 6 s until the maximum iteration is reached as the network size is very small. For the sensitivity analysis results in Section 4 with 30 nodes, the algorithm terminates due to the maximum computation time of 30 min for all cases.

#### 2.3.3. Charging decision algorithm

In this research, we calculate the deterministic decisions for the charging time and energy on a given route during the iterative solution search. When the modified route in the search is infeasible, we execute the charging decision algorithm (Algorithm 2) on the route as shown in line 14 of Algorithm 1. Given a route, its assigned vehicle and the network information, we modify the route by calculating the charging energy and time, considering the physical constraints on feasibility, such as the latest arrival time, travel and service time of the current route, initial and terminal energy level, the vehicle battery capacity, the charging power capacities of the vehicle battery and the chargers, and a fixed time to set up charging.

First, we set up the algorithm from line 1 to 3. If there is no charger on the route, then we return without modification because the algorithm does not add or remove locations to visit. The destinations with chargers and the detour chargers are added or removed by the destroy and insertion operators only, as described in Section 2.3.2. If any charger is on the route, we reset all charging time and energy.

Next, we calculate the available charging time on the route, $T_{max}$, considering the latest arrival time and the total travel time of the route from line 4 to 6. If no time is available, we return without modification. We calculate the target charging energy on the route, $E_{max}$, in line 8. We use the term 'target', because we want to charge as little as possible but make the route feasible with respect to the energy consumption. In calculating the energy consumption of the route, $E_{route}$, we consider the net consumption value because a downhill path can charge and increase the battery level from one node to another. We reflect the time-varying consumption as well. We finalize our $E_{max}$ value with respect to the initial, minimum, and terminal energy levels.

We initialize the total charging energy and time, $E$ and $T$, respectively to zero. From line 11 to 25, we calculate the charging decisions iteratively at the chargers in the visiting order on the route, while ensuring that the total charging energy and time do not exceed $E_{max}$ and $T_{max}$, respectively. At each charger on the route, we calculate the maximum charging energy and time at the charger as $e_j$ and $t_j$ concerning the physical constraints, like the charging power capacities of the vehicle and the charger, the elapsed time at the charger, the energy capacity of the vehicle, the energy level of the battery at the charger. If we find a nonzero $e_j$, we evaluate tentatively the travel time, energy consumption, and the OFV of the route in case we charge the vehicle by $e_j$. Note that a charging event may affect the entire route's travel costs, as it alters the time of arrivals at each location on the given route. If this charging improves the OFV of the route, we accept this decision and update the route with $t_j$ and $e_j$. We also update $E$ and $T$.

After iterating through the chargers on the route, we return the route with charging decisions. It is possible that the charging algorithm can be formulated as an optimization problem. However, the benefit of our deterministic charging decision is the fast computation time that does not hinder the efficiency of the meta-heuristic solver. This algorithm is designed as a modular component in the ALNS, as shown in line 14 of Algorithm 1 and can be easily improved.

#### 2.3.4. Travel cost estimation

We estimate the travel costs, i.e., travel time, energy consumption, and travel distance, for each edge between any pair of nodes in the network by an API serviced by WideSense. WideSense provides an AI software system that maximizes the operational performance of electric mobility. As a part of their engine, WideSense has developed and deployed a platform that delivers

**Algorithm 2:** Charging Decision Algorithm

**Input:** Information of a route, its assigned vehicle, network, and chargers
**Result:** A modified route with charging time and charging energy
/* Set up the route to modify */
**if** *there is no charger on the given route* **then**
  Terminate the algorithm and return the given route;
Remove all charging time and energy on the route;
/* Calculate the available charging time on the route */
$T_{max} = A^{-}\left(\overline{T^{v}}, T^{v}_{N+1} - T^{v}_{\emptyset}\right)$ ; // Latest arrival time subtracted by total travel time
**if** $T_{max} \leq 0$ **then**
  Terminate the algorithm and return the given route;
/* Calculate the target charging energy on the route */
Calculate total energy consumption on the route as $E_{route}$ ;
$E_{max} = \max\left(0, E_{route} - B^{v}_{ini} + \max\left(\underline{B^{v}}, B^{v}_{ter}\right)\right)$ ; // Target charging energy
/* Initialize */
Total charging energy on the route, $E \leftarrow 0$;
Total charging time on the route, $T \leftarrow 0$;
/* Calculate charging time and energy at each charger in order on the route */
**for** *each charger node* $j$ *on the route in the order of visit* **do**
  **if** $E < E_{max}$ *and* $T < T_{max}$ **then**
    $P_{max} = \min\left(\overline{P^{v}_{c}}, \overline{P^{j}_{n}}\right)$ ; // maximum charging power
    $e^{max}_{t} = P_{max} \cdot (T_{max} - T)$ ; // maximum charging energy regarding the available time
    $e^{max}_{c} = \overline{B^{v}} - E^{v}_{j}$ ; // maximum charging energy regarding the battery capacity and the battery level at node $j$
    $e_j = \min(E_{max} - E, e^{max}_{t}, e^{max}_{c})$;
    $t_j = e_j \cdot (P_{max})^{-1}$;
    **if** $e_j > 0$ **then**
      Calculate the time-varying travel time, energy consumption, and the OFV of the route, assuming we charge with $t_j$ and $e_j$ at this charger;
      **if** *The OFV of the route does not increase with* $t_j$ *and* $e_j$ **then**
        Update the route with $t_j$ and $e_j$;
        $E \leftarrow E + e_j$;
        $T \leftarrow T + t_j + \tau_f$;
  **else**
    Terminate the algorithm and return the given route;
Return the route;

high-precision energy consumption prediction for EVs and is tailored for real-time optimization. The platform leverages real-time data streams from vehicles' telematics, traffic, and weather forecasts and delivers tailored route and charging recommendations. Contextual prediction is obtained with highly accurate vehicle energy models that automatically learn from real-time vehicle sensor telemetry and other data streams, including slope, traffic forecasts, driver behavior, and weather.

The platform consists of two key elements: (a) physics-based vehicle performance models that capture the energy consumption and travel time on a per-vehicle, per-driver, per-road-segment basis, and (b) a data-driven learning algorithm that can estimate the parameters of the vehicle performance models to deliver high precision charge consumption estimation and charge depletion trajectories on routes for electrified vehicles. Using data, the platform can automatically learn from data over time. It can also adjust to the degradation characteristics of the vehicle components, including the drivetrain, battery, and motor.

In this work, we used WideSense API to compute high-precision estimates of charge depletion trajectories along a given route. In particular, for a given pair of nodes, date, and time, the WideSense API inquires the path of recommended roads from HERE API navigation. Based on the path, WideSense outputs the travel cost estimates for the given time. Note that we use HERE API navigation to find the path between two nodes as they provide a practical driving path in the real world. The input parameters used for the energy estimate API include the longitude and latitude coordinates of the origin and the destination, the departure time, the vehicle model, and the initial State of Charge of the vehicle battery. The API output includes, but is not limited to, the longitude and latitude coordinates of the travel path between the origin and the destination, the State of Charge, and the travel time along the path.

### *2.3.5. Performance evaluation*

The performance metrics include the total energy consumption in kWh, travel time in minutes, and travel distance in kilometers from the optimal routing solution from the proposed dispatching algorithm. For the field test, the energy measurement is the sum of the battery current multiplied by the battery voltage, and the logger sampling time interval is 0.1 s.

**Fig. 2.** Test vehicle: Hyundai Ioniq 5 (BEV).

For the analysis, we define the energy consumption difference and the travel time difference as $\Delta_e$ and $\Delta_t$ in percentages defined as:

$$\Delta_e = \frac{e_E - e_T}{e_T} \cdot 100\%, \tag{22}$$

$$\Delta_t = \frac{t_E - t_T}{t_T} \cdot 100\%, \tag{23}$$

where $e_E$ and $e_T$ are the energy consumption of the energy-minimizing route and the time-minimizing route, respectively, and $t_E$ and $t_T$ are the travel time of the energy-minimizing route and the time-minimizing route, respectively.

## 3. Field experiment

We solve the electric vehicle routing and charging problem using the solution framework in Section 2, and validate its energy saving impact in a real traffic network. In the following, we describe the methodology and the results of the field experiment.

### 3.1. Methodology

We design the field experiment to validate the energy consumption reduction from the dispatching algorithm, and assess the efficacy of the energy consumption estimation described in Section 2.3.4. The following briefly describes the test vehicle and the experiment setup.

#### 3.1.1. Test vehicle

We use a Hyundai IONIQ 5 shown in Fig. 2. The vehicle is installed with a data logger device, IPElog2 (IPETRONIK, 2023), and an auxiliary battery to power the logger. IPElog2 continuously records the vehicle's state during driving, charging, and idling at 0.1 Hertz frequency. The collected data includes odometer, speed, GPS coordinates, battery current, voltage, State of Charge, tire pressure, cabin temperature, and heating, ventilation, and airconditioning (HVAC) power consumption. The recorded data sets are automatically synchronized with the cloud server via WiFi and are easily accessible through the API provided by WideSense. Note that the test vehicle is instrumented with an autonomous driving hardware stack, including perception devices and computation devices, which is shown on the top of the vehicle for experimental purposes other than the current research. These features are not implemented in this study. Though the increase of frontal surface area and the vehicle mass may impact the vehicle's energy consumption, the field tests are conducted with the same vehicle condition with no difference of devices installed for all samples. The vehicle is charged with sufficient energy at the start of the experiment day, and there is no charging en-route during the field test cases.

#### 3.1.2. Experiment design

The field experiment is designed as follows. We define one sample as the traversal departing from the depot, visiting the destinations, and returning at the depot. We collect samples over 6 test dates, 2 traffic periods per date, and 2 test cases per traffic period, totaling 24 samples. The test dates only include weekdays. Two traffic periods are the evening peak (4 PM to 7 PM) and the off-peak (9 PM to midnight). Our baseline is the routing solution that minimizes the travel time, and the test case is the routing solution that minimizes total energy consumption. All samples are driven by a human driver who has attempted to drive under the

| Peak Traffic | | Off-peak Traffic | |
|---|---|---|---|
| **Travel Time Minimization** | **Energy Minimization** | **Travel Time Minimization** | **Energy Minimization** |
| Sample ID: 21 | Sample ID: 22 | Sample ID: 23 | Sample ID: 24 |

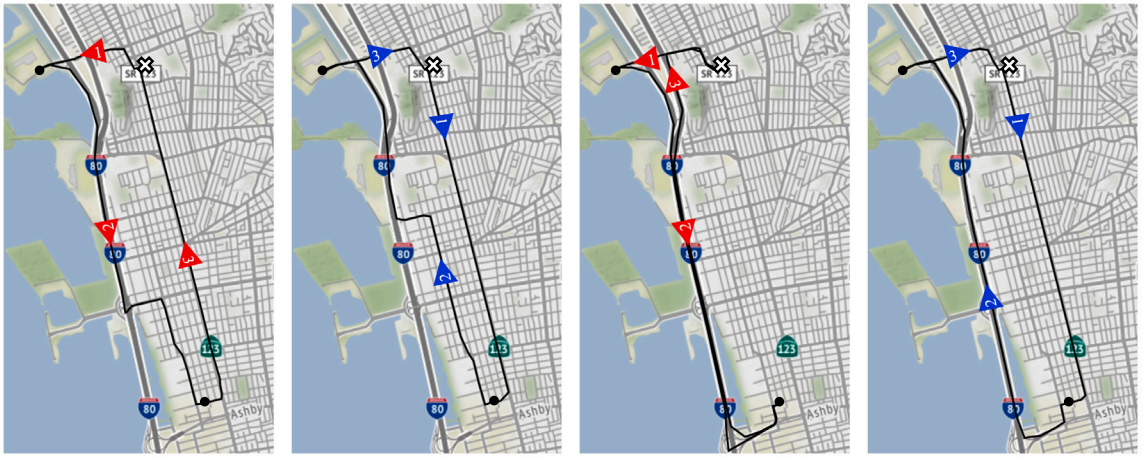


**Fig. 3.** GPS coordinates of field driving samples.

speed limit as closely as possible, not exceeding 10% deviation to the speed limit in free flow. At each destination, the vehicle is parked for two minutes. For all samples, the HVAC setting is maintained to keep the cabin interior at 70 degrees Fahrenheit with fan air speed at level 1, and the regeneration mode (selected as a feature in the vehicle) is kept at Level 1 (mode of least regeneration).

Notice that we only have one vehicle to test the baseline routing and our proposed routing. This means that we cannot drive both routing solutions at the same time in the same traffic conditions. However, even with two vehicles of identical specifications, the driving conditions would be different as the drivers in those two vehicles may have different driving behaviors. For instance, a more aggressive driver may consume more energy by severe braking and acceleration than the other driver. As aforementioned, we attempt to control the testing conditions as consistently as possible. Moreover, we reproduce the driving samples so that we can find statistically meaningful results.

We visit three supermarkets in the San Francisco East Bay Area, California, USA. One of them is considered a depot. The locations are chosen because of an easy access to their parking space, which allows consistent stopping locations at the destinations through repeated testing. Due to the small number of destinations in the routing, we can reduce the travel time of each sample and increase the number of sample sizes with various traffic conditions. Note that the locations are strategically chosen via preliminary simulation experiments to show sufficient evidence of energy savings from routing before the field test. In the Appendix D.1, we present additional simulation studies on a dispatching scenario with more destinations in a larger geographical region to show the routing performance. We visit three supermarkets in the San Francisco East Bay Area, California, USA. One of them is considered a depot. The locations are chosen because of easy access to their parking space, which enables stopping consistently at the same location for each destination through repeated testing. Due to the small number of destinations in the routing, we can reduce the travel time of each sample and increase the number of sample sizes with various traffic conditions. The locations are strategically chosen via preliminary simulation experiments to show sufficient evidence of energy savings from routing before the field test. In the Appendix D.1, we present additional simulation results for a scenario with more destinations to visit in a larger geographical region.

### *3.2. Results*

As a core part of the paper, this section provides evidence of the experiment with the GPS coordinates of driven route samples and proves that we can reduce energy consumption up to 31.4% when we drive the energy-minimizing routes compared to the time-minimizing routes. We investigate the mechanism of energy savings by analyzing the speed trajectories of driven routes.

#### *3.2.1. Driven route samples*

We present the GPS coordinates of driven route samples on the map; refer to Fig. 3. We have four figures — the left two figures during peak traffic and the right two figures during off-peak traffic. The baseline examples are the first and third figures with the time-minimizing routes, and the test examples are the second and fourth figures with the energy-minimizing routes. In the figures, the crosses indicate the depot, the arrows point to the travel direction, and the numbers in the arrows indicate the order of visits to the three locations in the routing solution. The most notable roads are Interstate 80 (I80) along the coast, which has speed limits up

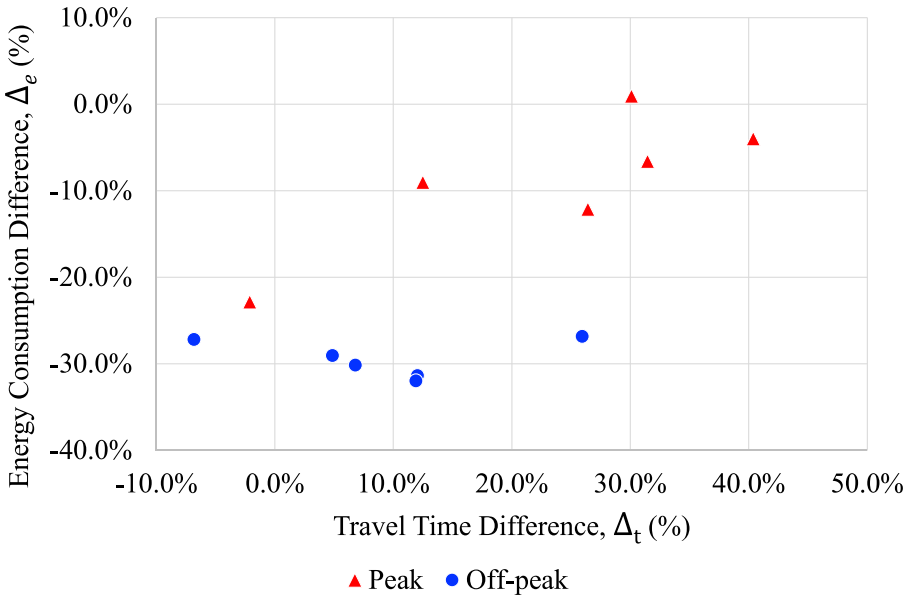


**Fig. 4.** Energy and travel time performance comparison of energy-minimizing routes to time-minimizing routes in the field, where the metrics are defined in Eqs. (22) and (23).

to 65 miles per hour (or about 105 km per h) in this area, and California State Route 123 (SR123), about 1 km from the shoreline, which has speed limits around 35 miles per hour (or about 55 km per hour) during the test dates.

As exemplified by these figures, the routing solutions for this particular dispatching problem use a similar collection of roads; however, they vary mainly on the travel direction (clock-wise or counter-clockwise on the map) and the amount of travel on the I80.

*3.2.2. Energy savings in the field*

We evaluate the energy consumption performance of the routing solution tested in the field; refer to Fig. 4, which succinctly presents the results. In the figure, the $x$-axis is the travel time difference, and the $y$-axis is the energy consumption difference. Out of 24 samples in the field, there are 12 baseline samples of the time-minimizing solution and 12 test samples of the energy-minimizing solution. We present 12 data points in the figure, each referring to the percentage difference between the baseline and the test case corresponding to the same date and traffic period. We categorize the samples into peak and off-peak traffic with triangles and circles, respectively. Note that a complete set of results is presented in Table 1 of Appendix B.

The key result of this paper is that we can significantly save energy with the proposed dispatching framework if we trade-off with travel time. We see that the energy-minimizing routes can reduce energy consumption up to 31.4% compared to the time-minimizing routes. The energy saving is more extensive in the off-peak period (around 25% to 30%) than in the peak period (around 0% to 20%). The trade-off is the travel time, where the energy-minimizing routes tend to travel longer, up to 40%.

The mechanism of how we save energy can be explained by the two right figures in Fig. 3. First, the energy-minimizing routes travel a shorter distance than the time-minimizing routes because the path between the depot and the destination in the bottom of the map is shorter via the arterial road (SR123) than the freeway (I80). Second, on the energy-minimizing routes, the vehicle drives at a lower speed on the arterial road than the freeway. The shorter and slower path in the energy-minimizing routes results in the energy savings.

The speed profiles of all samples in Fig. 5 provide further evidence of the mechanism of saving energy with a shorter distance and lower travel speed. The top and bottom figures present the results of peak and off-peak traffic, respectively. The $x$-axis is the distance traveled, and the $y$-axis is the wheel speed. The energy and time-minimizing routes are presented with black and gray lines, respectively. There is a similar trend in both peak and off-peak periods, where the energy-minimizing routes travel a shorter distance at a lower speed in general compared to the time-minimizing routes. The difference in travel distance and speed is more considerable in the off-peak period than in the peak period. During the peak, the traffic congestion results in slower speeds on the highway below 100 km/h, whereas during the off-peak, the speed on the highway maintains around 100 km/h consistently.

The energy savings are greater in the off-peak period, due to the significant difference in routing between the two routing cases in terms of the chosen road types, the travel distance, and consequently the travel speed. Note that in the field experiments, many random, unexpected, and uncontrollable events occurred on the road. These events, provided as a log in Appendix B.2, often caused the vehicle to deviate from the expected driving pattern of the solution. Against this randomness, however, we still claim strong evidence of energy savings; please refer to the hypothesis tests in Appendix C.

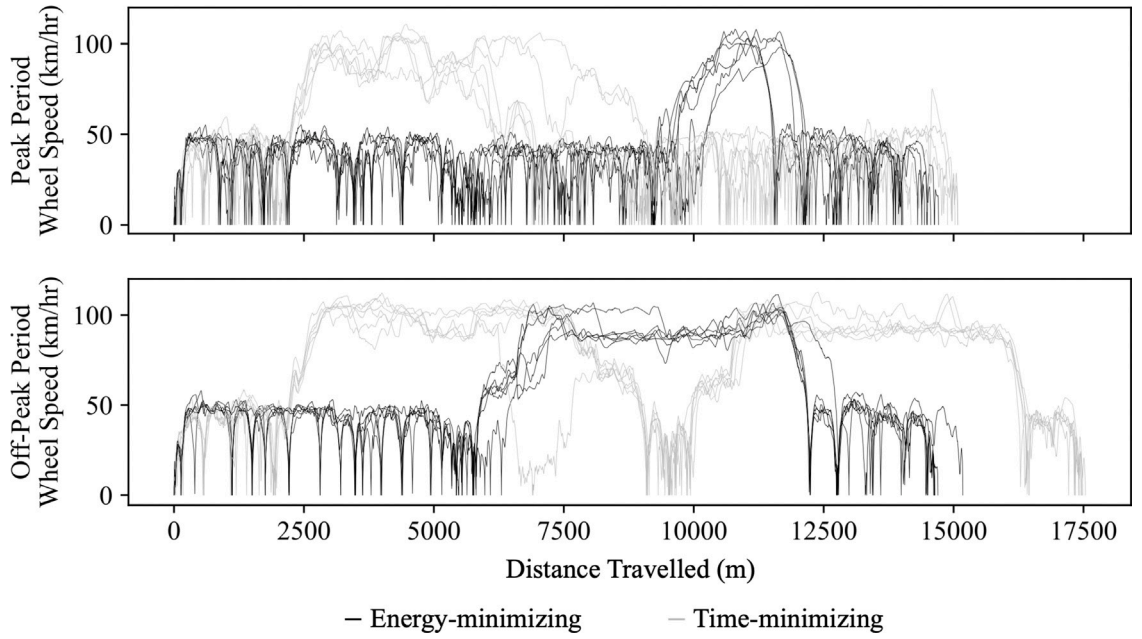


**Fig. 5.** Speed trajectory of driven routes against the travel distance.

## 4. Sensitivity analysis via simulation

In this section, we conduct a sensitivity analysis on the impact of several key constraints, namely the time and vehicle battery limits, on the energy consumption of the vehicle fleet. We choose to analyze the time limit because it implies what autonomous vehicles without human limits of driving hours can achieve. We consider adjusting the battery capacities to assess how the driving range impacts optimal routing and charging.

### *4.1. Methodology*

For this sensitivity analysis, we compare the energy-minimizing routing solutions of a given problem with varying parameters that constrain the fleet operation. We use the dispatching scenario with 30 destinations in the San Francisco Bay Area, where the vehicle can be dispatched (or the driver shift starts from) 9 AM. We add en-route chargers in addition to the depot chargers, because the solution is often infeasible without them in the geographical region of the network. We assumed slow chargers for destination at 6.6 kW and fast chargers for detour chargers at 250.0 kW. While the placement of the charger in the network is an important topic to discuss, our scope is on the efficient operation of the fleet rather than planning the charging network. Consequently, we omit further discussion on the siting of the charging infrastructure.

To analyze the time relaxation, we evaluate the routing performance of dispatching scenarios with varying driver's shift length (3 h to 23 h in 2-h increments). Equivalently, the drivers must return to the depot by their end of shift (12 PM to 8 AM in 2-h increments). We choose other parameters of the fleet so that they are not the binding constraints of the routing solution and that we isolate the impact of the time limit on the routing performance. The vehicle battery capacity is assumed to be 30 kWh, and the number of vehicles in the fleet is five. To analyze the battery capacity, we vary the battery sizes for all vehicles in the fleet from 15 kWh to 65 kWh in 5-kWh increments. The driver's shift is assumed to be long from 9 AM to 11 PM, to avoid the impact of time constraints on the routing result. For both analyses, we evaluate the total energy consumption in kWh and the total travel distance in km.

### *4.2. Results*

We find that relaxing the time limits of dispatching and increasing the battery capacities of vehicles can help find feasible solutions and reduce energy consumption. However, the gains in energy savings start to diminish around the current operation levels of fleets for the given scenario, telling us that we can achieve an energy-efficient operation immediately with currently available technologies. The following describes the results in detail.

#### *4.2.1. Time constraint relaxation on energy savings*

Often neglected in the VRP literature is the duration of a driver's maximum driving time, which is heavily regulated for safety in actual fleet operations. For instance, last-mile delivery drivers may have a shift that spans about 8 h per day, and long-haul drivers

| Driver shift | Short (9am – 2pm) | Long (9am – 10 pm) |
|---|---|---|
| Number of Vehicles used | 4 | 2 |
| Distance (km) | 466.0 km | 264.5 km |
| Time (min) | 1,056 min | 886 min |
| Energy (kWh) | 65.0 kWh | 36.5 kWh (−43.8%) |
| Route visualization<br>● : charger<br>● : depot<br>● : destination | 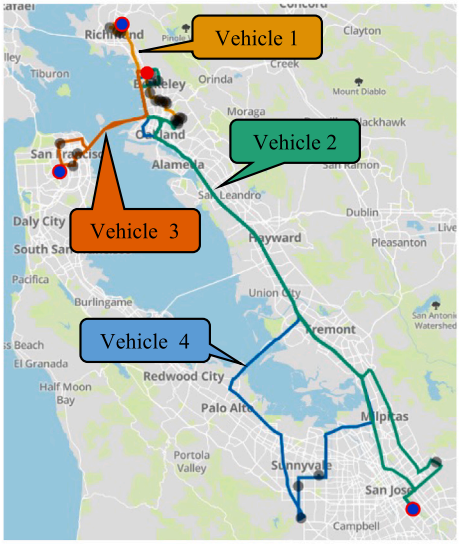 | 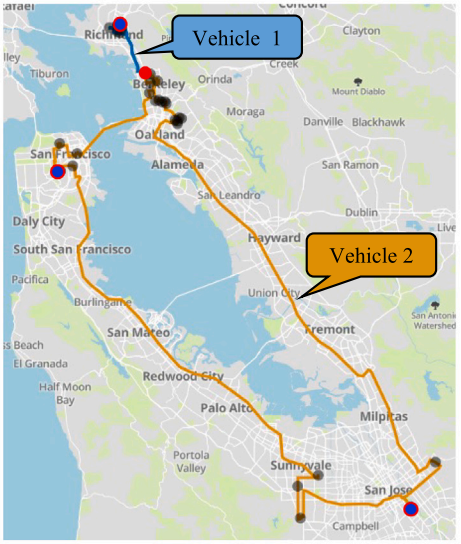 |

**Fig. 6.** Examples of time relaxation on energy consumption reduction.

may have a required break time, such as a 15-min break every 2 h of driving. This section describes a simulation experiment on the impact of time constraints on saving energy. Specifically, we vary the length of a driver's shift (the maximum driving time per vehicle) on the routing performance.

In Fig. 6, we illustrate the solutions of two cases of fleet dispatching — one with a short driver's shift of 5 h (9 AM to 2 PM) and another with a long driver's shift of 13 h (9 AM to 10 PM). As shown in the figure, the relaxed constraint on the driver's shift results in a routing solution with fewer vehicles dispatched, reduced deadheading distance, total distance traveled, and consequently reduced energy consumption.

We analyze the results further with a sensitivity analysis on the driver's shift. In Fig. 7, the left $y$-axis is the total energy consumption. The right $y$-axis is the total travel distance. The $x$-axis is the driver shift in hours. For each value of driver shift, we solved the problem three times with randomized initialization indicated by the cross marks. The lines show the trend through the average of three instances per shift length.

The solution is infeasible for the shift below 5 h for the given dispatching scenario. When we increase the shift length, we achieve feasibility and immediately see a significant drop in the energy consumption up to around 9 h of the driver shift. This drop is coincidental to the drop in the total travel distance. However, increasing the driver shift beyond 9 h shows a diminishing marginal return, where the energy consumption remains relatively constant. For this scenario, we can save energy significantly with our routing framework with human drivers with around 9 h of driving.

It is possible that, for a different dispatching scenario, the drop in energy consumption (indicated by the green arrow in the figure) may occur at a different driver shift value, perhaps around a longer shift hour that human drivers cannot operate. In the near future, autonomous vehicles may relax this time constraint and help reduce energy consumption by driving longer hours and reducing deadheading distance, though with a diminishing marginal return beyond a certain level of time relaxation.

#### *4.2.2. Battery capacity on energy savings*

There has been considerable effort to increase the battery capacity of EVs, as it helps increase the driving range and alleviate range anxiety, enabling accelerated EV adoption. In this section, we describe a sensitivity analysis of the impact of a vehicle battery's energy capacity in kWh ($\overline{B^p}$) on the routing performance. Note that we assume the change in battery capacity does not change the vehicle's energy efficiency. We acknowledge that this assumption is unrealistic because the battery mass may increase with a higher capacity, reducing the energy efficiency. We consider this factor and try to make conservative claims.

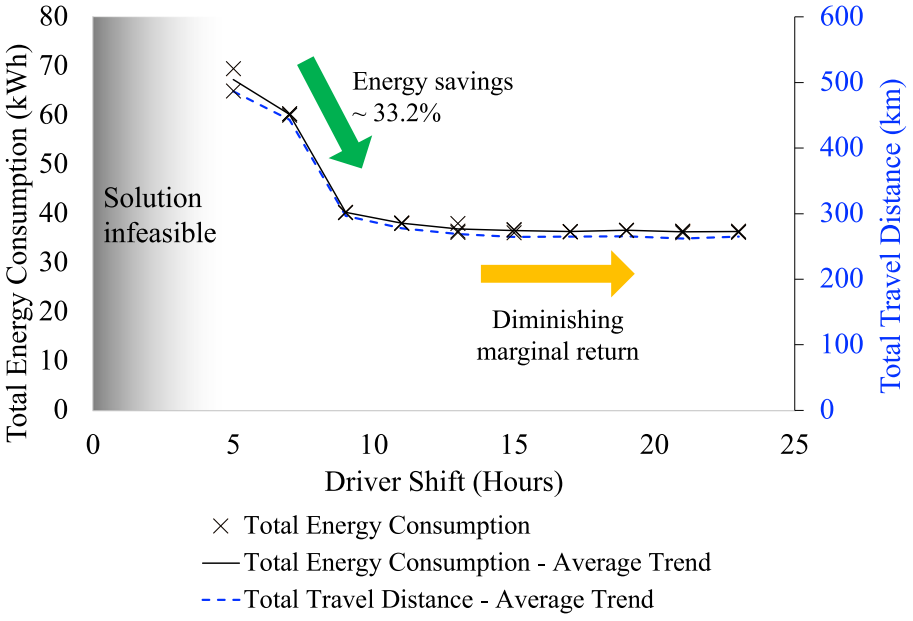


**Fig. 7.** Impact of time relaxation of dispatching on energy consumption.

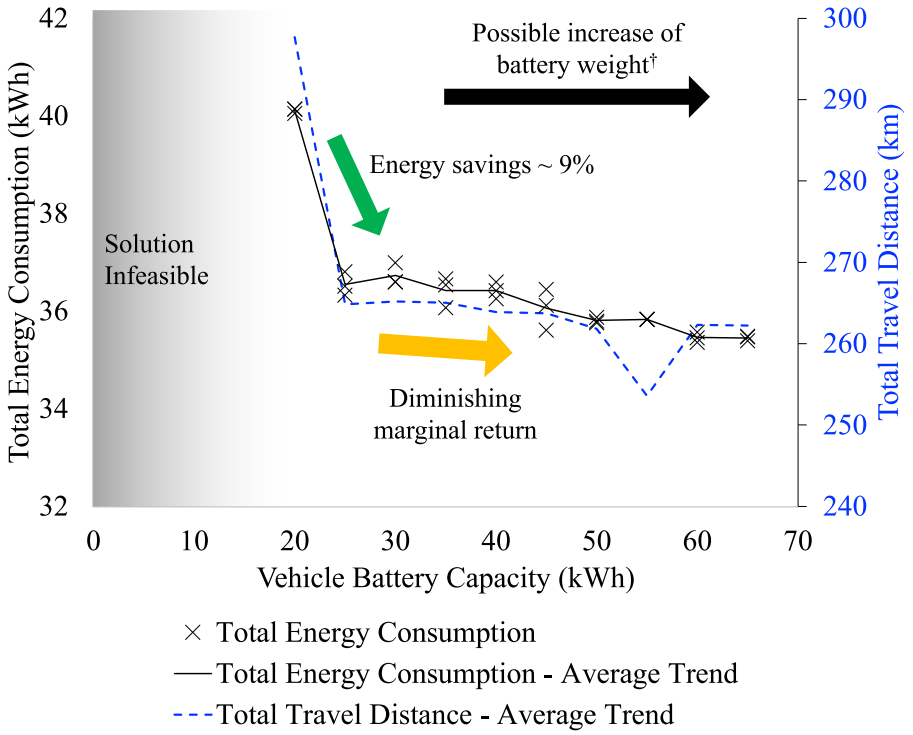


**Fig. 8.** Impact of vehicle battery capacity on energy consumption (†We assume the vehicle mass is constant as the vehicle battery capacity increases. This possibly overestimates the total energy consumption reduction, which means the marginal return may be even less for increasing the battery capacity.).

Similarly to Fig. 7, Fig. 8 has the left $y$-axis as the total energy consumption and the right $y$-axis as the total travel distance. The $x$-axis is the battery capacity in kWh for all vehicles used in the dispatching problem. For each battery capacity value, we solved the problem three times with randomized initialization, shown by the cross marks. The lines show the trend through the average of three instances per capacity value.

We first see that the vehicle battery must be a certain level, around 20 kWh for this given scenario, to produce a feasible solution. As the battery grows in capacity, the energy consumption drops significantly, coinciding with the drop in total travel distance. With a smaller battery capacity, each vehicle can drive a shorter distance and more vehicles must be dispatched to fulfill the trips. With a larger battery capacity, vehicles can travel longer distances and cover more destinations per vehicle, reducing the deadheading distance and the energy consumption. However, there is a diminishing marginal return beyond a capacity of around 25 kWh, as the total travel distance does not decrease much more. We are possibly overestimating the energy consumption reduction as the battery capacity increases because of the assumption of constant battery weight. Interpreting this result conservatively, the battery capacity improvement beyond a certain point may not save energy much more.

What we can learn from this analysis is that we can operate the electric fleets efficiently with the battery capacities currently available in the market and that an increase in battery capacities may not achieve such large gains as expected. This meaningful finding sheds light on the importance of efficiently operating the currently available technologies for energy-saving goals.

## 5. Discussion

In this paper, we develop a state-of-the-art solution framework to route and charge an electric vehicle fleet for minimal energy consumption, integrated with a high-precision prediction algorithm for energy consumption and travel time on real traffic networks. The core result is validating the energy consumption reduction in field experiments with a battery electric vehicle in the San Francisco Bay area. That is, we drive the energy-minimizing route through a given set of destinations and compare to the baseline time-minimizing route. The energy savings can reach up to 31.4%, and the savings are more significant in off-peak traffic than in peak traffic. This result is novel since no study has bridged the gap between the recent theory on vehicle routing solutions and the practical application. We prove the advantages of efficiently routing an electric vehicle fleet.

With this validation of the energy-efficient routing framework, we conduct a sensitivity analysis that investigates the impact of time and vehicle battery constraints. We find that extending the driver's shift length and the battery energy capacity helps expand the set of feasible solutions and reduce energy consumption. As the constraints are relaxed further, the energy saving diminishes in return. This result shows that we can immediately implement the efficient operation of the fleets to reduce their environmental footprint with the currently available technologies of vehicle batteries and human driving operation.

This work can be extended in multiple ways. First, significant uncertainty on the road can cause the dispatched vehicles to deviate from following the scheduled routing and charging decisions; refer to Appendix B.2. The prediction errors in travel time and energy consumption, though they tend to decrease as the travel distance increases, can impact the routing performance in real life. A robust routing algorithm must be developed and tested to capture the uncertainty on the road and to guarantee performance reliability. Also, when unexpected events occur and render a route infeasible, a real-time adjustment to the routing solution is necessary to mitigate this challenge and accomplish the fleet goals. For instance, a dispatched vehicle may break down unexpectedly and other operating vehicles can be re-routed to subsume the un-visited destinations of the broken vehicle. The real-time applications for wide adoption will require a method to forecast the traffic and vehicle systems and compute the efficient routing and charging schedules with a well-balanced performance of high accuracy and computation speed.

Second, the charging operation for electric fleets can have a large uncertainty impacting the success of vehicle dispatch in the real world. For example, uncertain waiting times at chargers, unreliable and unavailable chargers, power outages, and pricing issues can occur. This study did not validate the routing performance concerning charging operation in the field. The vehicles were sufficiently charged for the test driving. Also, our algorithm did not model the queuing at charging stations, impacting the successful completion of the trips. We must investigate the connected systems of mobility and energy and study the impact of charging infrastructure and power grid capacity on the efficiency of fleet operation. For instance, a database on the queuing times or the number of available chargers at different time of the day can be constructed. With this, we may formulate a stochastic optimization model with charging uncertainty, similar to Keskin et al. (2019). Field tests with en-route charging operations can shine a light on the impact of energy infrastructure to the logistics operation performance.

Third, we can expand this field experiment to other applications to urge the adoption of environmentally-conscious operation of vehicle fleets. Future topics may include routing to minimize the greenhouse gas emissions of non-electric vehicles and routing and charge scheduling to minimize the well-to-wheel emission of electric vehicles. In addition, the benefit-cost analysis of the environmentally-conscious operation can be conducted. For instance, we can investigate the economic benefit of autonomous electric vehicles that reduce energy consumption and energy costs by driving slowly and longer in the absence of labor costs.

Fourth, there are numerous factors that can impact the energy consumption of vehicle fleet operation, ranging from vehicle-level factors, such as air drag, vehicle mass, air conditioning, vehicle battery temperature, and driving behavior, infrastructure-level factors, such as road grade, pavement condition, and speed limits, to network-level factors, such as charger distribution, traffic congestion, and weather. While some of these factors are studied in this paper (such as route speed, travel distance, driver shift, charger distribution, and vehicle battery size) we can expand our sensitivity analysis and conduct an in-depth analysis on how these factors are intertwined to produce the final energy efficiency and provide specific guidelines on fleet operation for practical applications. To achieve this goal, it is essential to gather and process vast streams of data across various disciplines — from the traffic network, the service providers, the vehicles, the drivers, and more. Emerging artificial intelligence technologies, such as large models, are expected to hold significant potential in mobility solutions across their diverse disciplines (Qu et al., 2023). For instance, a novel language model was utilized to solve a delivery problem, illustrating its capability to depict the implicit driver knowledge and behaviors in real-world scenarios (Liu et al., 2023).

Fifth, despite the rapid adoption of EVs, the current logistics industry still uses non-electric or hybrid electric vehicles. Therefore, we can model the energy consumption of other vehicle types for efficient routing and demonstrate the environmental benefits for the immediate application of the proposed framework for various vehicle types.

## CRediT authorship contribution statement

**Soomin Woo:** Writing – review & editing, Writing – original draft, Visualization, Validation, Software, Methodology, Investigation, Formal analysis, Conceptualization. **Eric Yongkeun Choi:** Writing – review & editing, Writing – original draft, Methodology, Investigation, Formal analysis, Conceptualization. **Scott J. Moura:** Writing – review & editing, Supervision, Project administration, Methodology, Funding acquisition, Formal analysis, Conceptualization. **Francesco Borrelli:** Writing – review & editing, Supervision, Project administration, Funding acquisition, Formal analysis, Conceptualization.

## Declaration of competing interest

The authors declare the following financial interests/personal relationships which may be considered as potential competing interests: Francesco Borrelli reports a relationship with WideSense that includes: board membership, consulting or advisory, employment, and equity or stocks. If there are other authors, they declare that they have no known competing financial interests or personal relationships that could have appeared to influence the work reported in this paper.

## Data availability

Data will be made available on request.

## Acknowledgments

This material is based upon work partially supported by ARPA-E NEXTCAR Program - DE-AR000079. Any opinions, findings, conclusions or recommendations presented in this material are only those of the authors and do not necessarily reflect the views of ARPA-E. Francesco Borrelli has financial interests in WideSense, Inc.

## Appendix A. Heuristic operators

We list the heuristic operators borrowed from the literature and describe additional operators we propose newly in this paper. Note that this paper defines zones to group nodes in the network. To define the zones, we use k-means clustering on the latitudes and longitudes of the nodes. We choose the number of zones, $k$ by the Elbow Criterion.

*Initial solution.* We produce the initial solution by the greedy insertion of destinations, often used in the literature (Keskin and Çatay, 2016; Demir et al., 2012; Emeç et al., 2016; Keskin et al., 2019).

*Destroy operators.* We use random, worst-time, Shaw, proximity-based, demand-based, and zone methods to remove destinations and random route removal method (Keskin and Çatay, 2016; Demir et al., 2012; Emeç et al., 2016; Keskin et al., 2019). In addition, we propose the following heuristics.

*Worst energy destination removal:* This operator modifies the worst-time removal heuristic and removes the destinations from the solution based on their energy consumption from the preceding node to the succeeding node. The removal process is otherwise the same as the worst-time heuristic.

*Random detour charger removal:* This operator randomly chooses and removes detour chargers from the solution. For the number of detour chargers to remove, we randomly choose an integer less than or equal to the number of detour chargers in the solution.

*Worst energy detour charger removal:* This operator chooses and removes the detour chargers in the solution in the order of the decreasing energy consumption from the preceding destination to the succeeding destination. For the number of detour chargers to remove, we randomly choose an integer less than or equal to the number of detour chargers in the solution.

*Least visiting route removal:* This operator chooses and removes the routes in the solution in the order of the increasing number of destinations to visit. We use the $\omega$ number used in Keskin and Çatay (2016) for the number of routes to remove.

*First/second half route removal:* This drastic operator removes the first or second half of destinations visited by all routes in the solution.

*Each vehicle type route removal:* This drastic operator removes one random route for each vehicle type. If a vehicle type is not used in the solution and has no destinations to visit, nothing changes for that vehicle type.

*Switch vehicle type:* This operator randomly chooses one vehicle each from two vehicle types, switches their routing decisions, and resets the charging decisions. This heuristic is helpful when the vehicles in the fleet have heterogeneous characteristics, for example, 10 kWh and 30 kWh battery capacities. We do not remove any route or destinations from the solution, but the vehicle type switch can perturb the solution search and make it infeasible. Therefore, we consider it a destroy operator.

*Repair operators.* We insert the destinations to the route using greedy methods based on the route's total travel time (Keskin and Çatay, 2016; Keskin et al., 2019). We use randomized greedy insertion based on the route's total travel time, where we randomly choose one out of the three best candidates of insertion. We also use total energy consumption to evaluate the repair performance for the greedy and the randomized greedy methods.

Similar to the greedy station insertion (Keskin et al., 2019), we use greedy method to insert detour chargers on the route. Also, we use zone-based detour charger insertion, which is a modification of the zone insertion (Demir et al., 2012). This operator randomly selects a zone and adds a detour charger in the zone with the best objective function value. If the zone has no detour charger, we continue to randomly select a zone until there is a detour charger.

**Table 1**
Comprehensive results of the field experiment.

| Sample ID | | Test date | Traffic period | Energy consumption (kWh) | | | Travel time (min) | | | Travel distance (km) | | | Route speed (km/h) | | |
|---|---|---|---|---|---|---|---|---|---|---|---|---|---|---|---|
| E | T | | | E | T | Δ | E | T | Δ | E | T | Δ | E | T | Δ |
| 1 | 2 | 09/28/22 | Peak | 2.11 | 2.09 | 0.9%[a] | 45.8 | 35.2 | 30.1% | 14.9 | 17.7 | −15.8% | 19.5 | 30.2 | −35.3% |
| 6 | 5 | 09/30/22 | Peak | 1.96 | 2.23 | −12.1% | 46.4 | 36.7 | 26.4% | 15.0 | 15.1 | −0.7% | 19.4 | 24.7 | −21.4% |
| 9 | 10 | 10/03/22 | Peak | 2.51 | 2.62 | −4.0% | 43.1 | 30.7 | 40.4% | 14.9 | 17.8 | −16.3% | 20.7 | 34.8 | −40.4% |
| 14 | 13 | 10/04/22 | Peak | 1.94 | 2.52 | −22.9% | 37.3 | 38.1 | −2.1% | 14.2 | 14.6 | −2.7% | 22.8 | 23.0 | −0.7% |
| 17 | 18 | 10/05/22 | Peak | 2.08 | 2.29 | −9.0% | 43.2 | 38.4 | 12.5% | 14.9 | 17.7 | −15.8% | 20.7 | 27.7 | −25.2% |
| 22 | 21 | 10/06/22 | Peak | 2.03 | 2.17 | −6.6% | 44.7 | 34.0 | 31.5% | 14.7 | 15.3 | −3.9% | 19.7 | 27.0 | −26.9% |
| 3 | 4 | 09/28/22 | Off-peak | 2.03 | 2.95 | −31.4% | 28.8 | 25.7 | 12.1% | 14.9 | 17.8 | −16.3% | 31.0 | 41.6 | −25.3% |
| 8 | 7 | 09/30/22 | Off-peak | 2.14 | 3.02 | −29.1% | 25.8 | 24.6 | 4.9% | 15.3 | 15.4 | −0.6% | 35.6 | 37.6 | −5.3% |
| 11 | 12 | 10/03/22 | Off-peak | 2.25 | 3.22 | −30.2% | 26.7 | 25.0 | 6.8% | 17.7 | 14.8 | 19.6% | 39.8 | 35.5 | 12.0% |
| 16 | 15 | 10/04/22 | Off-peak | 2.15 | 3.17 | −32.0% | 26.3 | 23.5 | 11.9% | 15.3 | 14.9 | 2.7% | 34.9 | 38.0 | −8.2% |
| 19 | 20 | 10/05/22 | Off-peak | 2.32 | 3.17 | −26.8% | 29.6 | 23.5 | 26.0% | 17.8 | 14.3 | 24.5% | 36.1 | 36.5 | −1.2% |
| 24 | 23 | 10/06/22 | Off-peak | 2.22 | 3.06 | −27.2% | 27.4 | 29.4 | −6.8% | 14.4 | 14.2 | 1.4% | 31.5 | 29.0 | 8.8% |

E: Energy minimizing route sample.
T: Travel time minimizing route sample (baseline).
$\Delta = \frac{(E-T)}{T} \cdot 100\%$.

[a] This sample was collected on an unusually hot day. With the consistent setting of AC at 70 degrees Fahrenheit, the total AC energy was consumed significantly more especially for the energy-minimizing route with a longer travel time. The energy consumption without the HVAC energy, which was recorded separately by the logger, was 1.95 kWh for the energy-minimizing route and 1.98 kWh for the time-minimizing route. In other words, the energy consumption of energy-minimizing route was slightly less (by 1.79%) without the HVAC energy than that of the time-minimizing route.

## Appendix B. Field experiment results

In this section of the appendix, we present the complete statistics on the field experiment samples and the log of notable traffic events in the field that may have affected the results.

### *B.1. Complete results of the field experiments*

The complete results from the field experiment are presented below in Table 1. We consider one sample as the driving of one routing solution, totaling 24 samples. We categorize the results in traffic periods — peak and off-peak. We indicate the results of energy-minimizing and time-minimizing routes with E and T, respectively. The values under $\Delta$ indicate the percentage difference between energy-minimizing and time-minimizing routes, similarly to Eqs. (22) and (23).

Note that the sample IDs are given in the order of the sample collection. On each day and each period, one time-minimal route and one energy-minimal route were collected. However, traffic congestion can change dramatically over a short span of time, especially during the evening peak. Therefore, the field experiments alternated between the time-minimal and energy-minimal routes to test first each day. For example on 09/28/22, the energy-minimal route was collected (sample ID: 1) before the time-minimal route (sample ID: 2). On 09/30/22, the energy-minimal route was collected (sample ID: 6) after the time-minimal route (sample ID: 5). For the results during the peak period on 09/28/2022, the energy consumption of the energy-minimizing route was larger than the time-minimizing route due to the unexpectedly high ambient temperature and HVAC energy consumption. Its detailed explanation is given in the footnote of the Table.

### *B.2. Log of unexpected events during the field experiments*

The traffic and driving conditions can be highly random in the real world, and we observed many events that may have impacted our field results. We briefly list the events that occurred during our field experiments.

- On 09/28/2022, the ambient temperature was very high and the HVAC consumed more energy. Note that the temperature setting of AC was consistently at 70 degrees Fahrenheit for all tests.
- On 09/30/2022, during the energy-minimizing route traversal in the peak period, the traffic was halted for a train passing for a few minutes, increasing travel time significantly.
- On 10/04/2022, during the time-minimizing route traversal in the peak period, double-parked vehicles on San Pablo Avenue caused traffic congestion, significantly increasing travel time.
- On 10/05/2022, a road closure on Heinz Avenue impacted both travel-minimizing and energy-minimizing routes in the peak period, as well as the energy-minimizing route in the off-peak period. A detour route was driven as close to the solution as possible. Also, during the energy-minimizing route in the off-peak period, the defog AC feature was used for about one minute.
- On 10/06/2022, during the time-minimizing route traversal in the off-peak period, two left-most lanes were closed on the freeway for road work, causing severe congestion and stop-and-go traffic.

## Appendix C. Hypothesis testing on saving energy

As described in Appendix B.2, there is significant randomness on the road, which may challenge our claim on reducing energy consumption with our algorithm in the field. To strengthen our claim against the uncertainty, we present hypothesis testing results as the following. We use student t-tests because we compare the means of two cases (the time-minimizing and the energy-minimizing), and the tests are one-sided because we compare if one is greater than the other. For the tests, we use the random variables defined as the following.

- $e_T$: The energy consumption of time-minimizing route during the peak or the off-peak period (kWh)
- $e_E$: The energy consumption of energy-minimizing route during the peak or the off-peak period (kWh)

In the following, we conduct a test with the following null and alternative hypotheses, therefore testing if the energy-minimizing route uses less energy than the time-minimizing route.

- $H_0 : e_E \geq e_T$
- $H_A : e_E < e_T$

### C.1. Test 1: Off-peak period

First, we conduct a hypothesis test for the off-peak period. We have six samples each for time-minimizing and energy-minimizing routes, totaling 12 samples. The degree of freedom is 10. The T-statistic is 15.447 and the P-value is $1.318e{-}08$. Therefore, we reject the null hypothesis at 99% probability. In other words, the energy-minimizing routes consume less energy compared to the time-minimizing routes.

### C.2. Test 2: Peak period

Second, we conduct a hypothesis test for the peak period. We have six samples each for time-minimizing and energy-minimizing routes, totaling 12 samples. The degree of freedom is 10. The T-statistic is 1.792 and the P-value is 0.0517. Therefore, we reject the null hypothesis only at 90%.

## Appendix D. Additional findings from simulation studies

In this section, we present interesting findings from simulation studies that complement the sensitivity analysis in the main manuscript.

### D.1. Routing in a larger geographical region

The field tests in this study span a relatively small geographical region shown in Fig. 3 to reduce the testing time and increase the sample size with the available testing resources. In this section, we present some simulated routing results that span a large geographical region that also shows stark differences in routing solutions when minimizing different objective functions, similar to the case of the field test.

Fig. 9 shows that the routing results significantly differ in the travel direction and selected roads. The vehicles start their trips at 4 PM with afternoon traffic congestion. The two results show the routing solution with different objective functions. The time-minimizing route dispatches the vehicle to the highways, such as I580, I680, and I280, with a larger circumference counter-clockwise. This routing avoids the congestion in the inner highways, taken by the energy-minimizing route in the clockwise direction, such as I880 and SR101. The different selection of travel directions and roads change the total distance, the energy consumption, and the travel time.

### D.2. Driving range of electric vehicles on energy savings

We briefly describe an interesting finding on the impact of using vehicles of various driving ranges on energy-efficient routing. Since BEVs with a long driving range are costly, one may consider using plug-in hybrid EVs (PHEVs) as a solution with a longer range but poorer energy efficiency.

| Objective | Travel Time Minimization | Energy Minimization |
|---|---|---|
| Energy (kWh) | 30.0 | 26.9 (−10.3%) |
| Time (min) | 247.7 | 259.8 (+4.9%) |
| Distance (km) | 210.0 | 199.7 (−4.9%) |
| Route visualization<br>#: traversal order | 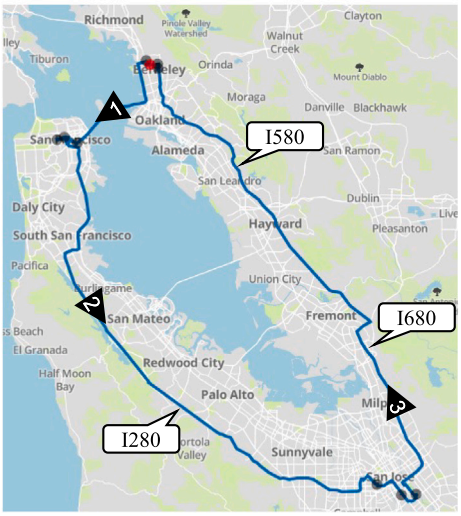 | 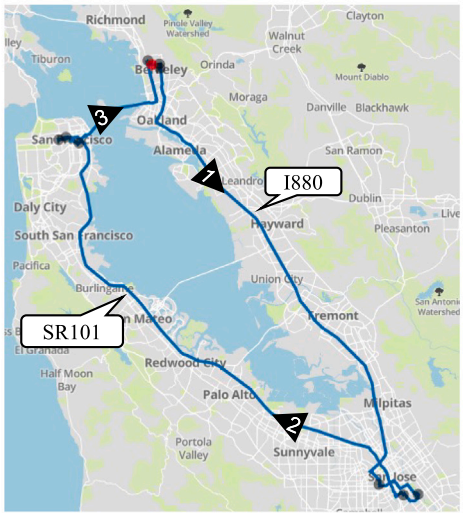 |

**Fig. 9.** Routing solutions of a larger geographical region.

| Available Fleet | 0 BEV, 4 PHEVs | 1 BEV, 3 PHEVs |
|---|---|---|
| Vehicles Used | 2 Total (2 PHEVs) | 3 Total (1 BEV, 2 PHEVs) |
| Energy (kWh) | 58.0 kWh | 44.4 kWh (−23.5%) |
| Time (min) | 750 min | 1,032 min (+37.6%) |
| Distance (km) | 262.1 km | 305.4 km (+16.5%) |
| Route visualization<br>: charger<br>: depot<br>: destination |  | 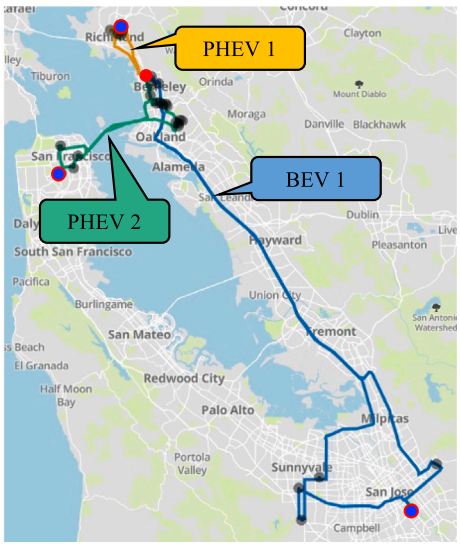 |

**Fig. 10.** Routing solutions with longer-range vehicles with lower energy efficiency.

In this short thought experiment, we compare the routing solutions of different fleet compositions; refer to Fig. 10. In one case, we have no BEVs but four PHEVs. In the other case, we introduce one BEV and use three PHEVs. With the change of one vehicle type, we save energy by 23.5%, even though we dispatch three vehicles in total and travel 16.5% longer distance due to deadheading. This simple experiment assumes that the PHEVs consume energy 1.8 times more than the BEVs, accordingly to the rough estimates from the field data collected by WideSense.

What is interesting is that in the case of one BEV and three PHEVs, the PHEVs are used only for short trips due to lower energy efficiency, while the charger in the network increases the range of BEVs. This is ironic because the longer-range PHEVs travel short distances, if possible. The PHEVs would be used at a high energy cost if the solution is infeasible only with BEVs, however, we argue that installing an en-route charger will achieve feasible solutions with BEVs at higher energy efficiency than using PHEVs.

## References


Amazon, 2022. Amazon's electric delivery vehicles from rivian roll out across the U.S.. URL: https://www.aboutamazon.com/news/transportation/amazons-electric-delivery-vehicles-from-rivian-roll-out-across-the-u-s.

Asghari, M., Al-e-hashem, S.M.J.M., 2021. Green vehicle routing problem: A state-of-the-art review. Int. J. Prod. Econ. 231, 107899. http://dx.doi.org/10.1016/j.ijpe.2020.107899.

Bahrami, S., Nourinejad, M., Amirjamshidi, G., Roorda, M.J., 2020. The plugin hybrid electric vehicle routing problem: A power-management strategy model. Transp. Res. C 111, 318–333. http://dx.doi.org/10.1016/j.trc.2019.12.006.

Basso, R., Kulcsár, B., Egardt, B., Lindroth, P., Sanchez-Diaz, I., 2019. Energy consumption estimation integrated into the electric vehicle routing problem. Transp. Res. D 69, 141–167. http://dx.doi.org/10.1016/j.trd.2019.01.006.

Basso, R., Kulcsár, B., Sanchez-Diaz, I., 2021. Electric vehicle routing problem with machine learning for energy prediction. Transp. Res. B 145, 24–55. http://dx.doi.org/10.1016/j.trb.2020.12.007.

Basu, A.K., Tatiya, S., Bhattacharya, S., 2018. Overview of electric vehicles (EVs) and EV sensors. In: Energy, Environment, and Sustainability. Springer Singapore, pp. 107–122. http://dx.doi.org/10.1007/978-981-13-3290-6_7.

Bruglieri, M., Paolucci, M., Pisacane, O., 2023. A matheuristic for the electric vehicle routing problem with time windows and a realistic energy consumption model. Comput. Oper. Res. (ISSN: 0305-0548) 157, 106261. http://dx.doi.org/10.1016/j.cor.2023.106261.

Butler, K., Ehsani, M., Kamath, P., 1999. A matlab-based modeling and simulation package for electric and hybrid electric vehicle design. IEEE Trans. Veh. Technol. 48 (6), 1770–1778. http://dx.doi.org/10.1109/25.806769.

Catay, B., Keskin, M., 2017. The impact of quick charging stations on the route planning of electric vehicles. In: 2017 IEEE Symposium on Computers and Communications. ISCC, IEEE, http://dx.doi.org/10.1109/iscc.2017.8024521.

Demir, E., Bektaş, T., Laporte, G., 2012. An adaptive large neighborhood search heuristic for the pollution-routing problem. European J. Oper. Res. 223 (2), 346–359. http://dx.doi.org/10.1016/j.ejor.2012.06.044.

Department of Energy, 2022a. Where the energy goes: Electric cars. URL: https://www.fueleconomy.gov/feg/atv-ev.shtml.

Department of Energy, 2022b. Where the energy goes: Gasoline vehicles. URL: https://www.fueleconomy.gov/feg/atv.shtml.

Department of Energy, 2023a. All-electric vehicles - fuel economy. URL: https://www.fueleconomy.gov/feg/evtech.shtml#:~:text=EVs%20convert%20over%2077%25%20of,Environmentally%20friendly%20.

Department of Energy, 2023b. Electric vehicles for fleets. URL: https://afdc.energy.gov/vehicles/electric_fleets.html.

Elshaer, R., Awad, H., 2020. A taxonomic review of metaheuristic algorithms for solving the vehicle routing problem and its variants. Comput. Ind. Eng. 140, 106242. http://dx.doi.org/10.1016/j.cie.2019.106242.

Emeç, U., Çatay, B., Bozkaya, B., 2016. An adaptive large neighborhood search for an E-grocery delivery routing problem. Comput. Oper. Res. 69, 109–125. http://dx.doi.org/10.1016/j.cor.2015.11.008.

Ferro, G., Paolucci, M., Robba, M., 2018. An optimization model for electrical vehicles routing with time of use energy pricing and partial recharging. IFAC-PapersOnLine 51 (9), 212–217. http://dx.doi.org/10.1016/j.ifacol.2018.07.035.

Guanetti, J., Kim, Y., Borrelli, F., 2019. Eco-routing of connected plug-in hybrid electric vehicles. In: 2019 IEEE 58th Conference on Decision and Control. CDC, IEEE, http://dx.doi.org/10.1109/cdc40024.2019.9030078.

Hiermann, G., Hartl, R.F., Puchinger, J., Vidal, T., 2019. Routing a mix of conventional, plug-in hybrid, and electric vehicles. European J. Oper. Res. 272 (1), 235–248. http://dx.doi.org/10.1016/j.ejor.2018.06.025.

IPETRONIK, 2023. PIElog2. URL: https://www.ipetronik.com/en/products-services/data-loggers/ipelog2-2.html.

Keskin, M., Çatay, B., 2016. Partial recharge strategies for the electric vehicle routing problem with time windows. Transp. Res. C 65, 111–127. http://dx.doi.org/10.1016/j.trc.2016.01.013.

Keskin, M., Laporte, G., Çatay, B., 2019. Electric vehicle routing problem with time-dependent waiting times at recharging stations. Comput. Oper. Res. 107, 77–94. http://dx.doi.org/10.1016/j.cor.2019.02.014.

Kim, Y.J., Chung, B.D., 2023. Energy consumption optimization for the electric vehicle routing problem with state-of-charge-dependent discharging rates. J. Clean. Prod. (ISSN: 0959-6526) 385, 135703. http://dx.doi.org/10.1016/j.jclepro.2022.135703.

Kopfer, H., Vornhusen, B., 2018. Energy vehicle routing problem for differently sized and powered vehicles. J. Bus. Econom. 89 (7), 793–821. http://dx.doi.org/10.1007/s11573-018-0910-z.

Koyuncu, I., Yavuz, M., 2019. Duplicating nodes or arcs in green vehicle routing: A computational comparison of two formulations. Transp. Res. E 122, 605–623. http://dx.doi.org/10.1016/j.tre.2018.11.003.

Kucukoglu, I., Dewil, R., Cattrysse, D., 2021. The electric vehicle routing problem and its variations: A literature review. Comput. Ind. Eng. 161, 107650. http://dx.doi.org/10.1016/j.cie.2021.107650.

Lin, B., Ghaddar, B., Nathwani, J., 2021. Electric vehicle routing with charging/discharging under time-variant electricity prices. Transp. Res. C 130, 103285. http://dx.doi.org/10.1016/j.trc.2021.103285.

Liu, Y., Wu, F., Liu, Z., Wang, K., Wang, F., Qu, X., 2023. Can language models be used for real-world urban-delivery route optimization? Innovation (ISSN: 2666-6758) 4 (6), 100520. http://dx.doi.org/10.1016/j.xinn.2023.100520.

Lu, J., Chen, Y., Hao, J.-K., He, R., 2020. The time-dependent electric vehicle routing problem: Model and solution. Expert Syst. Appl. 161, 113593. http://dx.doi.org/10.1016/j.eswa.2020.113593.

Macrina, G., Laporte, G., Guerriero, F., Pugliese, L.D.P., 2019. An energy-efficient green-vehicle routing problem with mixed vehicle fleet, partial battery recharging and time windows. European J. Oper. Res. 276 (3), 971–982. http://dx.doi.org/10.1016/j.ejor.2019.01.067.

Moghdani, R., Salimifard, K., Demir, E., Benyettou, A., 2021. The green vehicle routing problem: A systematic literature review. J. Clean. Prod. 279, 123691. http://dx.doi.org/10.1016/j.jclepro.2020.123691.

Montoya, A., Guéret, C., Mendoza, J.E., Villegas, J.G., 2017. The electric vehicle routing problem with nonlinear charging function. Transp. Res. B 103, 87–110. http://dx.doi.org/10.1016/j.trb.2017.02.004.

Nunzio, G.D., Gharbia, I.B., Sciarretta, A., 2021. A general constrained optimization framework for the eco-routing problem: Comparison and analysis of solution strategies for hybrid electric vehicles. Transp. Res. C 123, 102935. http://dx.doi.org/10.1016/j.trc.2020.102935.

Peng, D., Wu, G., Boriboonsomsin, K., 2023. Energy-efficient dispatching of battery electric truck fleets with backhauls and time windows. SAE Int. J. Electr. Veh. (ISSN: 2691-3755) 13 (1), http://dx.doi.org/10.4271/14-13-01-0009.

Qu, X., Lin, H., Liu, Y., 2023. Envisioning the future of transportation: Inspiration of ChatGPT and large models. Commun. Transp. Res. (ISSN: 2772-4247) 3, 100103. http://dx.doi.org/10.1016/j.commtr.2023.100103.

Vidal, T., Laporte, G., Matl, P., 2020. A concise guide to existing and emerging vehicle routing problem variants. European J. Oper. Res. 286 (2), 401–416. http://dx.doi.org/10.1016/j.ejor.2019.10.010.

Zhang, W., Liu, J., Wang, K., Wang, L., 2024a. Routing and charging optimization for electric bus operations. Transp. Res. E (ISSN: 1366-5545) 181, 103372. http://dx.doi.org/10.1016/j.tre.2023.103372.

Zhang, L., Liu, Z., Yu, B., Long, J., 2024b. A ridesharing routing problem for airport riders with electric vehicles. Transp. Res. E (ISSN: 1366-5545) 184, 103470. http://dx.doi.org/10.1016/j.tre.2024.103470.